Comput Geosci (2012) 16:93–122
DOI 10.1007/s10596-011-9255-1

ORIGINAL PAPER

A penalty mechanism for discontinuous Galerkin processing of Darcy velocity

Jean-Baptiste Apoung Kamga

Received: 1 December 2010 / Accepted: 1 September 2011 / Published online: 27 October 2011

Abstract The Darcy velocity plays an important role in the flow in porous media, particularly when a miscible displacement is concerned. One major requirement when approximating this velocity is the continuity of its normal component. The discontinuous Galerkin methods, by nature, are not well designed for this challenge, since approximations are performed in space of totally discontinuous polynomials. We propose in such context a penalty approach, in order to enhance the continuity of the normal component of the Darcy velocity. The resulting formulation is shown to be stable whatever the origin of the pressure but requires the inversion of a global matrix. We then propose two modifications leading to the inversion of only local matrices. Error estimates are furnished and the analysis of the penalty parameter vis-a-vis the computed pressure is addressed. We show that the proposed reconstructions have better performance compared to the simple local differentiation of the computed pressure. Numerical tests are provided to illustrate the theoretical results.

Keywords Darcy flow · Discontinuous Galerkin method · Darcy velocity post-processing · Penalty formulation

Mathematics Subject Classifications (2010) 65N12 · 65N30

J.-B. Apoung Kamga (✉)
Laboratoire de Mathématiques, UMR 8628,
Univ Paris-Sud, Orsay 91405, France
e-mail: jean-baptiste.apoung@math.u-psud.fr

J.-B. Apoung Kamga
CNRS, Orsay 91405, France

1 Introduction

The flow computation in porous media amounts to seek the distribution of the pressure and that of the Darcy velocity over the media. It often happens that the computed velocity is coupled with transport in porous media. Consequently at the computational level, the numerical method needs to produce an accurate velocity.

In the discontinuous Galerkin (DG) approximation theory [2, 3, 17], two types of formulation are used. The first is the mixed formulation in which the velocity and the pressure are computed simultaneously (see [10, 12–16, 18, 22]). The second is the primal formulation where the problem is transformed into a single one over the pressure (see [5, 10, 12, 26–28, 30]), and the velocity is obtained by a post-processing technique. Unluckily, flow computation in real life involves huge spatial domain and long time calculation. This unfortunately requires not only intensive computing, which are memory consuming, but also efficiency in the computation of the Darcy velocity. A good trade-off between memory consummation and efficiency in computing the Darcy velocity is the primal formulation if an efficient post-processing velocity technique is available. Unfortunately, obtaining better velocity approximations is not a simple task. A requirement for the Darcy velocity is to possess continuous normal component [7]. Most post-processing techniques associated to primal DG formulation involve the so-called *lifting operators* (see for instance [10, 12–16, 18, 21–23]). Using this *lifting operators*, the velocity is sought in a space of totally discontinuous functions, which may result in a computed velocity with a poor continuous normal component at the interface between two sub-domains. An alternative

was shown to resort to a projection into conformal finite element spaces. Following this idea, Bastian and Rivière, see [7], require the Brezzis–Douglas–Marini (BDM) space projection (see [11]), to derive a local H-div projection. This projection only requires the cell-to-cell computation of discontinuous Galerkin velocity and ensures the continuity of the mean value of the velocity across the interfaces. However, not all information on the primal equation are used. Therefore, Ern et al. [19] found it efficient to use the pressure equation and consequently the DG fluxes for post-processing the velocity. This led them to require the Raviart Thomas finite element space [25]. Since all conformal finite elements suffer from instability when distorted elements are used [24], we find it necessary to still use the discontinuous Galerkin approximation of the velocity and to efficiently enforce the continuity of the normal component of the Darcy velocity across the interfaces between elements by a penalty approach. This is motivated by the fact that best methods on distorted elements are those capable of getting rid of the reference element. This is exactly one power of the DG formulations (see the concluding remark in [30]). The only requirement in such elements reduces to defining efficient quadrature formula. This is possible because distorted elements can be decomposed into simplexes over which efficient quadrature formula are available.

In this paper, we present three velocity post-processing techniques and compare them to a simple local differentiation procedure. All these reconstructions make use in their analysis of all the properties of the primal formulation but possess independent interpretations which endowed them with advantageous properties. They are a kind of stabilization at the discrete level of the continuous level lifting operators. With the first reconstruction, optimal error estimates are provided. This reconstruction is well designed for enforcing the continuity of the normal component of the velocity. The price to pay is that the associated matrix is not block-diagonal. Hence, we further propose two modifications ensuring the same optimal convergence rate in L^2 norm and in the L^∞ norm of the jump of the normal component of the velocity. These reconstructions allow for a local-to-one-cell computation of the velocity; these are still better than the simple local-in-the-cell differentiation even though they are less efficient than the previous. Numerical results are provided which validate the errors estimate analysis and compare the three reconstructions with the simple local-in-the-cell differentiation of the pressure.

The good theoretical and numerical behavior of the three reconstruction procedures is due to specificity of the computed pressured. A specific control, by the help of some parameters, of the jump of the pressure and the jump of its normal derivative should be possible (see in the preliminary section below). These assumptions can affect the penalty parameter in the reconstructed velocity. Several primal DG formulations automatically satisfy those stability constraints, and a specific one is pointed out in the preliminary section of the this paper. We therefore analyze the stability parameter in all reconstruction and show that only that of the second reconstruction is dependent on the stability property of the formulation used to compute the pressure. We therefore supply explicit bounds on the stability parameter in this case.

The paper is organized as follows: In Section 2, the model equation and notations are presented, then followed in Section 3 by some assumptions on the computed pressure, necessary for the error estimates and the stability analysis of the proposed velocity reconstructions. In Section 4, we present and analyze three reconstruction techniques. Numerical validations of the error estimates and the comparison of the different reconstructions are addressed in Sections 5 and 6. The conclusions of our analysis is presented in Section 7.

2 Model problem and notations

2.1 Model problem

Let $\Omega \subset \mathcal{R}^d$, $d = 2, 3$ be an open-bounded convex and polygonal domain with Lipschitz boundary. We consider the following problem:

$$\begin{cases} -\nabla \cdot (K\nabla p) = f & \text{in} \quad \Omega, \\ p = p_{\mathrm{D}} & \text{on} \quad \Gamma_{\mathrm{D}}, \\ (K\nabla p)\cdot \mathbf{n} = g_{\mathrm{N}} & \text{on} \quad \Gamma_{\mathrm{N}}, \end{cases} \tag{1}$$

where Γ_{N} and Γ_{D} denote the Dirichlet and Neumann parts of the boundary $\partial\Omega$, respectively, $\bar{\Gamma}_{\mathrm{D}} \cup \bar{\Gamma}_{\mathrm{N}} = \partial\Omega$ and $\Gamma_{\mathrm{D}} \cap \Gamma_{\mathrm{N}} = \emptyset$. Here, $\mathbf{n}$ represents the unit normal vector external to $\partial\Omega$. We suppose that the Dirichlet part of the boundary is not empty and has positive $(d-1)$-Lebesgue measure ($|\Gamma_{\mathrm{D}}| > 0$), $f \in L^2(\Omega)$, $p_{\mathrm{D}} \in H^{1/2}(\Gamma_{\mathrm{D}})$, $g_{\mathrm{N}} \in L^2(\Gamma_{\mathrm{N}})$. We assume that $K = (K_{i,j})_{1\le i,j\le d} \in (L^\infty(\Omega))^{d,d}$ is a symmetric positive definite tensor, satisfying

$$\begin{aligned} 0 < \lambda_m|\zeta|^2 &\le \sum_{i,j=1}^{d} K_{ij}(x)\zeta_i\zeta_j \\ &\le \lambda_M|\zeta|^2 < \infty, \quad x \in \Omega, 0 \ne \zeta \in \mathcal{R}^d, \end{aligned} \tag{2}$$

where λ_m and λ_M are non-negative real numbers. We introduce for any subset $E \subset \Omega$ two non-negative real numbers λ_m^E and λ_M^E such that

$$0 < \lambda_m^E |\zeta|^2 \leq \sum_{i,j=1}^{d} K_{ij}(x)\zeta_i\zeta_j$$
$$\leq \lambda_M^E |\zeta|^2 < \infty, \quad x \in E, 0 \neq \zeta \in \mathcal{R}^d. \tag{3}$$

Equation 1 models a permanent flow in a porous media, where p denotes the hydrodynamic pressure. Under specific conditions that we will assumed herein, this problem has a unique solution with sufficient regularity allowing to compute some first-order derivatives of p (see for instance [1, 9, 20]). Consequently, it is often common to compute the quantity

$$\mathbf{u} = -K\nabla p \tag{4}$$

called the Darcy velocity which plays important role in transport in porous media (see [6–8, 19, 26]).

When the solution of Eq. 1 has been obtained using specific discretization method, then the problem of approximating the solution of Eq. 4 in a given space is referred to as post-processing of the Darcy velocity in that space. This is called post-precessing because the simple differentiation through formula (4) will not give satisfactory result, namely for non-polynomial K, the result will not even be polynomial.

In the present paper, we aim at post-processing the Darcy velocity in the space of totally discontinuous polynomials because efficient discontinuous Galerkin method for computing Eq. 1 is available. Therefore, if we could compute the Darcy velocity using the DG method, we would then reduce considerably the implementation and the computational effort when solving coupled flow and transport in porous media.

However, it is well-known in such coupling that a minimal requirement for the Darcy velocity is to belong to the space of vectorial functions, each component of which is in $L^2(\Omega)$ and whose divergence falls in $L^2(\Omega)$, namely the space $H_{\text{div}}(\Omega)$. This is achieved in broken space settings provided that the normal trace of $\mathbf{u}$ is continuous across the interfaces between subsets of Ω. Because DG fails within the broken-space setting, our strategy will be to use penalty approach for enforcing the continuity of the normal component of the velocity.

We give three different formulations, two of which are modification of the first one with the purpose of reducing the computational effort as well as the dependency of the stability parameter vis-a-vis the computed pressure. Let us point out that the computed pressure is subject to a stability constraint involving some specifics parameters. It will be user-prone that this constraint does not affect the stability parameter in the post-precessing of the Darcy velocity.

2.2 Definitions and notations

Let τ_h , with $h > 0$, be a possibly non-conforming finite partition of Ω into elements $\{E\}$ with Lipschitz boundary ∂E. We associate with any element $E \in \tau_h$ its measure $|E|$, its diameter $h_E = \max_{x,y\in E} |x - y|$, and assume that $h = \max_{E\in\tau_h} h_E$. The partition τ_h is assumed to be *regular* in the sense that any element $E \in \tau_h$ is convex and there exists a constant $\rho > 0$ such that the ball of radius ρh_E is contained in each simplex obtained by connecting vertices of E. The partition τ_h is also assumed to be *quasi-uniform*, i.e., there exists a constant $\tau > 0$ such that $\frac{h}{h_E} < \tau$ for all $E \in \tau_h$. We associate with τ_h the set of interior faces denoted by $\xi_h^{'}$ and the set of boundary faces denoted ξ_h^{∂}, both defined as

$$\xi_h^{'} = \left\{e = \partial E \cap \partial E', \text{mes}(\partial E \cap \partial E') > 0\right\},$$
$$\xi_h^{\partial} = \left\{e = \partial E \cap \partial\Omega, \text{mes}(\partial E \cap \partial\Omega) > 0\right\}.$$

The set of all faces is referred to as $\xi_h = \xi_h^{'} \cup \xi_h^{\partial}$. Moreover, to account for boundary conditions, we further split the boundary faces as follows $\xi_h^{\partial} = \xi_h^{\text{D}} \cup \xi_h^{\text{N}}$ where,

$$\xi_h^{\text{D}} = \left\{e = \partial E \cap \Gamma_{\text{D}}, \text{mes}(\partial E \cap \Gamma_{\text{D}}) > 0\right\},$$
$$\xi_h^{\text{N}} = \left\{e = \partial E \cap \Gamma_{\text{N}}, \text{mes}(\partial E \cap \Gamma_{\text{N}}) > 0\right\}.$$

For any element $E \in \tau_h$, the outward unit normal vector on ∂E is denoted by $\mathbf{n}$. We also associate with any $e \in \xi_h$ a unit normal vector $\mathbf{n}_e$ which coincides with the outward unit normal vector to $\partial\Omega$ if $e \in \xi_h^{\partial}$.

For any integer s and non-empty subset $S \subset \Omega$ where S can either be Ω or any element of τ_h or ξ_h, we denote by $H^s(S)$ the usual Sobolev space endowed with the usual norm $\|\cdot\|_{s,S}$. If $S = \Omega$, we simply write $\|\cdot\|_s$. We define the broken space $H^s(\tau_h)$ as

$$H^s(\tau_h) = \left\{v \in L^2(\Omega); v|_E \in H^s(E), \quad \forall E \in \tau_h\right\} \tag{5}$$

and the finite element approximation space $\mathcal{V}_h^k \subset H^s(\tau_h)$ for any $k \geq 1$ as

$$\mathcal{V}_h^k = \left\{v \in L^2(\Omega); v|_E \in \mathcal{P}_k(E), \quad \forall E \in \tau_h\right\}, \tag{6}$$

where $\mathcal{P}_k(E)$ is the set of polynomial functions of degree k on E. Since the order of the polynomial approximation can vary over elements of τ_h, we denote by k_E the order of this approximation on element $E \in \tau_h$. Therefore, the superscript k in notation $\mathcal{V}_h^k$ will stand

for the minimal value of k_E over all elements $E \in \tau_h$. We will also use thee following space:

$$\Sigma_h^k = \left(\mathcal{V}_h^k\right)^d. \tag{7}$$

Since the broken space contains discontinuous functions, it is necessary to define the jumps and the means of functions in $H^s(\tau_h), s \geq 2$. Let then $u \in H^s(\tau_h), s \geq 2$, and $e \in \xi_h^{'}$ shared by two elements E and E'. Let $\mathbf{n}_e$ be the unit normal vector on e, directed from E to E'. The jump of u on e, denoted by $[\![v]\!]$, and the mean of v on e, denoted by $\{v\}$, are defined as

$$[\![v]\!] = (v|_E)|_e - (v|_{E'})|_e, \quad \{v\} = \frac{(v|_E)|_e + (v|_{E'})|_e}{2}. \tag{8}$$

where $v|_E$ stands for the restriction of v on E. If v is a vector-valued function, its jumps and means are obtained by applying the definition to each component of v.

In the sequel, we adopt the following convention: Any internal face is shared by two elements denoted E and E', and we simply write the restriction of any function v on those elements as v and v', respectively. The unit normal vector $\mathbf{n}_e$ is supposed to be outward to E, i.e., $\mathbf{n}_e = \mathbf{n} = -\mathbf{n}'$, such that the jump and the mean of v on e simply read $[\![v]\!] = v - v'$, $\{v\} = \frac{v+v'}{2}$.

We will need the following inverse trace inequality due to Warburton and Hesthaven [31].

Lemma 1 (Inverse inequality) *Let $E \in \tau_h$ be a subset of $\mathbb{R}^d$ and $q \in \mathcal{P}_k(E)$. Then*

$$\|q\|_{0,e} \leq \sqrt{\frac{(k+1)(k+d)}{d}\frac{|e|}{|E|}}\,\|q\|_{0,E} \quad \forall e \subset \partial E, \tag{9}$$

where $|e|$ and $|E|$ denote the measure of e and E, respectively.

We will also assume the following interpolation property taking from [29].

Lemma 2 (Approximation) *Let $E \in \tau_h$ and $p \in H^s(E)$. There exists a constant C independent of p, k, h_E and a sequence of polynomials $\hat{p}_k \in \mathcal{P}_k(E), k = 1, 2\cdots$, such that*

$$\|p - \hat{p}_k\|_{r,E} \leq C\frac{h_E^{\mu-r}}{k^{s-r}}\|p\|_{s,E}, \quad 0 \leq r < \mu,$$

$$\|p - \hat{p}_k\|_{r,e} \leq C\frac{h_E^{\mu-r-\frac{1}{2}}}{k^{s-r-\frac{1}{2}}}\|p\|_{s,E}, \quad 0 \leq r < \mu - \frac{1}{2}, \tag{10}$$

where $\mu = \min(k+1, s)$ and $e \subset \partial E$.

With all these descriptions at hands, let us now point some assumption on the approximated pressure from which the Darcy velocity will be derived.

3 Preliminaries

The post-precessing of the velocity presented in this paper although capable of providing good solutions whenever the origin of the pressure will require some assumptions on the computed pressure in order to enable the a priori error estimate for that velocity. Henceforth, we will assume that the pressure has been computed in such a way that the following holds:

Let $p \in H^1(\Omega) \cap H^s(\tau_h)$, with $s \geq 2$ be the solution of Eq. 1 and $p_h \in \mathcal{V}_h^k$, $k \geq 2$ be the computed approximation of p; then there exists a constant $C > 0$ independent of k, h such that

$$|\!|\!| p - p_h |\!|\!|^2 \leq C\frac{h^{2\mu-2}}{k^{2s-3}}\sum_{E\in\tau_h}\|p\|_{s,E}^2, \tag{11}$$

where $\mu = \min(k+1, s)$ and

$$|\!|\!| \eta |\!|\!|^2 = B(\eta,\eta) + J^{\beta_h}(\eta,\eta) + H^{\beta_h}(\eta,\eta) + H_{BN}^{\beta_h}(\eta,\eta) + M^{\beta_h}(\eta,\eta), \tag{12}$$

with

$$\beta_h = \sigma\frac{k^2}{h}, \quad \sigma > 0, \tag{13}$$

$$B(p,q) = \sum_{E\in\tau_h}\int_E K\nabla p\cdot\nabla q\,\mathrm{d}x, \tag{14}$$

$$J^{\beta}(p,q) = \sum_{e\in\xi_h^{'}}\frac{\beta}{2}\int_e [\![p]\!][\![q]\!]\,\mathrm{d}\gamma + \sum_{e\in\xi_h^{\mathrm{D}}}\beta\int_e pq\,\mathrm{d}\gamma, \tag{15}$$

$$H^{\beta}(p,q) = \sum_{e\in\xi_h^{'}}\frac{1}{2\beta}\int_e [\![(K\nabla p)\cdot\mathbf{n}_e]\!][\![(K\nabla q)\cdot\mathbf{n}_e]\!]\,\mathrm{d}\gamma, \tag{16}$$

$$H_{BN}^{\beta}(p,q) = \sum_{e\in\xi_h^{\mathrm{N}}}\frac{1}{\beta}\int_e (K\nabla p)\cdot\mathbf{n}_e\,(K\nabla q)\cdot\mathbf{n}_e\,\mathrm{d}\gamma, \tag{17}$$

$$M^{\beta}(p,q) = \sum_{e\in\xi_h^{'}}\frac{2}{\beta}\int_e \{(K\nabla p)\cdot\mathbf{n}_e\}\{(K\nabla q)\cdot\mathbf{n}_e\}\,\mathrm{d}\gamma + \sum_{e\in\xi_h^{\mathrm{D}}}\frac{1}{\beta}\int_e (K\nabla p)\cdot\mathbf{n}_e(K\nabla q)\cdot\mathbf{n}_e\,\mathrm{d}\gamma. \tag{18}$$

With parameter β_h in Eq. 13 selected such that there exist a constant C^* depending only on $f, P_{\mathrm{D}}, g_{\mathrm{N}}$ such that

$$\| p_h \| \leq C^*(f, P_{\mathrm{D}}, g_{\mathrm{N}}). \tag{19}$$

In the rest of the paper, β will denote this value of β_h.

Let us point out that several primal discontinuous Galerkin methods satisfy the assumption (11) as stated in the remark below.

Remark 1

- The assumption (11) and (19) is fulfilled by almost all primal discontinuous Galerkin methods, such as NIPG, SIPG, and IIPG for sufficient large value of the stability parameter $\sigma > 0$. This amount to select β carefully such that Eq. 19 holds. This is an a posteriori computation since that value may differ from that used to compute the pressure.
- Because of the above constraint, we point out here a primal DG formulation of problem (1) which straightforwardly satisfy Eqs. 11 and 19. This formulation which is studied in detail in Apoung Kamga (submitted for publication) is given by:

$$\begin{cases} \text{seek} \quad p_h \in \mathcal{V}_h^k \text{ such that } \forall q_h \in \mathcal{V}_h^k \\ \mathcal{A}_h(p_h, q_h) = \mathcal{L}_h(q_h). \end{cases} \tag{20}$$

with

$$\begin{aligned} \mathcal{A}_h(p_h, q_h) = {} & B(p_h, q_h) - J(p_h, q_h) + \varepsilon J(q_h, p_h) \\ & + J^{\beta_h}(p_h, q_h) + H^{\beta_h}(p_h, q_h) \\ & + H_{BN}^{\beta_h}(p_h, q_h), \end{aligned} \tag{21}$$

$$\begin{aligned} \mathcal{L}_h(q_h) = {} & L(q_h) + L_{\mathrm{N}}(q_h) + J_{\mathrm{D}}(q_h) \\ & + \varepsilon J_D^{\beta_h}(q_h) + H_{\mathrm{N}}^{\beta_h}(q_h), \end{aligned} \tag{22}$$

where ($\varepsilon = 1$) for non-symmetric version and ($\varepsilon = -1$) for symmetric version, and

$$\begin{aligned} J(p, q) = {} & \sum_{e \in \xi_h^{'}} \int_e \{(K\nabla p) \cdot \mathbf{n}_e\} [\![q]\!] \, \mathrm{d}\gamma \\ & + \sum_{e \in \xi_h^{\mathrm{D}}} \int_e (K\nabla p) \cdot \mathbf{n}_e \, q \, \mathrm{d}\gamma, \end{aligned} \tag{23}$$

$$H_{\mathrm{N}}^{\beta}(q) = \sum_{e \in \xi_h^{\mathrm{N}}} \frac{1}{\beta} \int_e g_{\mathrm{N}} (K\nabla q) \cdot \mathbf{n}_e \, \mathrm{d}\gamma, \tag{24}$$

$$\begin{aligned} J_{\mathrm{D}}(q) &= \sum_{e \in \xi_h^{\mathrm{D}}} \int_e p_{\mathrm{D}} (K\nabla q) \cdot \mathbf{n}_e \, \mathrm{d}\gamma \\ J_{\mathrm{D}}^{\beta}(q) &= \sum_{e \in \xi_h^{\mathrm{D}}} \beta \int_e p_{\mathrm{D}} q \, \mathrm{d}\gamma, \end{aligned} \tag{25}$$

$$\begin{aligned} L(q) &= \sum_{E \in \tau_h} \int_E f q \, \mathrm{d}x, \\ L_{\mathrm{N}}(q) &= \sum_{e \in \xi_h^{\mathrm{N}}} \int_e g_{\mathrm{N}} q \, \mathrm{d}\gamma. \end{aligned} \tag{26}$$

4 Post-processing of the Darcy velocity

The lifting operators [10, 12–16, 18, 21–23] are the common procedures to derive the approximate Darcy velocity from the computed pressure. Because they are designed to assure stability property to the DG formulation of the pressure equation, they may not give satisfactory velocity, unless high-order polynomials are used when computing the pressure. However, for large domain computation, this should be avoided since high-order polynomials are more memory consuming. For this reason, we propose some specific velocity reconstructions, namely Eqs. 27, 31, and 37, based on penalty approach. The presentation of these reconstructions are organized as follows: We present in Section 4.1 the first post-processing technique and its a priori error estimates and penalty parameter analysis. Progressively, in Sections 4.2 and 4.3, we give two modifications of the first reconstruction to make the computation less expensive and address their error estimates and stability analysis.

4.1 First velocity reconstruction approach

To determine the Darcy velocity, we propose the following problem:

$$\begin{cases} \text{Find } \mathbf{u}_h \in \Sigma_h^k \text{ such that } \forall \mathbf{v}_h \in \Sigma_h^k, \\ \displaystyle\sum_{E \in \tau_h} \int_E K^{-1} \mathbf{u}_h \cdot \mathbf{v}_h \, \mathrm{d}x + \sum_{e \in \xi_h^{'}} \frac{1}{2\alpha} \int_e [\![\mathbf{u}_h \cdot \mathbf{n}_e]\!] [\![\mathbf{v}_h \cdot \mathbf{n}_e]\!] \, \mathrm{d}\gamma \\ \quad + \displaystyle\sum_{e \in \xi_h^{\mathrm{N}}} \frac{1}{\alpha} \int_e (\mathbf{u}_h \cdot \mathbf{n}_e)(\mathbf{v}_h \cdot \mathbf{n}_e) \, \mathrm{d}\gamma \\ \quad = - \displaystyle\sum_{E \in \tau_h} \int_E \mathbf{v}_h \cdot \nabla p_h \, \mathrm{d}x + \sum_{e \in \xi_h^{'}} \int_e [\![p_h]\!] \{\mathbf{v}_h \cdot \mathbf{n}_e\} \, \mathrm{d}\gamma \\ \qquad + \displaystyle\sum_{e \in \xi_h^{\mathrm{D}}} \int_e (p_h - p_{\mathrm{D}})(\mathbf{v}_h \cdot \mathbf{n}_e) \, \mathrm{d}\gamma \\ \qquad - \displaystyle\sum_{e \in \xi_h^{\mathrm{N}}} \frac{1}{\alpha} \int_e (g_{\mathrm{N}})(\mathbf{v}_h \cdot \mathbf{n}_e) \, \mathrm{d}\gamma. \end{cases} \tag{27}$$

Proposition 1 *Let p_h be a computed approximation of the solution $p \in H^s(\tau_h), s \geq 2$ of Eq. 1 satisfying the estimations (11). There exists a unique solution u_h of problem (27). Moreover, if $\mathbf{u} = -K\nabla p$ and $\alpha = \frac{\sigma k^2}{h}$, then there exists a constant C independent of h and k such that*

$$\sum_{E\in\tau_h} \|\mathbf{u}-\mathbf{u}_h\|^2_{0,E} \leq C\frac{h^{2\mu-2}}{k^{2s-3}}\left(\sum_{E\in\tau_h}\|\mathbf{u}\|^2_{s,E}+\sum_{E\in\tau_h}\|p\|^2_{s,E}\right), \tag{28}$$

$$\sum_{e\in\xi_h'} \|[\![(\mathbf{u}-\mathbf{u}_h)\cdot\mathbf{n}_e]\!]\|^2_{0,e} + \sum_{e\in\xi_h^{\mathrm{N}}} \|(\mathbf{u}-\mathbf{u}_h)\cdot\mathbf{n}_e\|^2_{0,e} \leq C\frac{h^{2\mu-3}}{k^{2s-5}}\left(\sum_{E\in\tau_h}\|\mathbf{u}\|^2_{s,E}+\sum_{E\in\tau_h}\|p\|^2_{s,E}\right), \tag{29}$$

where $\mu = \min(k+1, s)$.

Proof See Appendix 1. □

4.1.1 Estimation of the stability parameter

We address in this section the potential dependence of the penalty parameter α with respect to the penalty parameter β. We claim here that there is no relationship between the penalty parameter α, in the problem (27), and the stability parameter β in Eq. 12. More precisely the following holds:

Proposition 2 *Let p_h be the approximate solution of Eq. 1 satisfying Eq. 11 and β the parameter in Eq. 12. For any penalty parameter α in formulation (27), there exists a constant $C > 0$ independent of β such that*

$$\sum_{E\in\tau_h}\int_E K^{-1}\mathbf{u}_h\cdot\mathbf{u}_h\,\mathrm{d}x + \sum_{e\in\xi_h'}\frac{1}{\alpha}\int_e [\![\mathbf{u}_h\cdot\mathbf{n}_e]\!]^2\,\mathrm{d}\gamma + \sum_{e\in\xi_h^{\mathrm{N}}}\frac{1}{\alpha}\int_e(\mathbf{u}_h\cdot\mathbf{n}_e)^2\,\mathrm{d}\gamma \leq CC^*(f, P_{\mathrm{D}}, g_{\mathrm{N}}). \tag{30}$$

Proof See Appendix 5. □

4.2 Second velocity reconstruction approach

It appears in formulation (27) that the resulting matrix is not block-diagonal. A less computational effort will be obtained if one can tune the formulation in order to obtain a block-diagonal matrix where each diagonal block is associated with a single cell. This is the aim of this sub-section. After some trials, we propose the following formulation:

$$\begin{cases} \text{Find } \mathbf{u}_h \in \Sigma_h^k \text{ such that } \forall \mathbf{v}_h \in \Sigma_h^k \\ \displaystyle\sum_{E\in\tau_h}\int_E K^{-1}\mathbf{u}_h\cdot\mathbf{v}_h\,\mathrm{d}x + \sum_{e\in\xi_h^{\mathrm{N}}}\frac{1}{\alpha}\int_e \mathbf{u}_h\cdot\mathbf{n}_e\mathbf{v}_h\cdot\mathbf{n}_e\,\mathrm{d}\gamma \\ \quad = -\displaystyle\sum_{E\in\tau_h}\int_E \mathbf{v}_h\cdot\nabla p_h\,\mathrm{d}x + \sum_{e\in\xi_h'}\int_e [\![p_h]\!]\{\mathbf{v}_h\cdot\mathbf{n}_e\}\,\mathrm{d}\gamma \\ \qquad + \displaystyle\sum_{e\in\xi_h^{\mathrm{D}}}\int_e (p_h - p_{\mathrm{D}})(\mathbf{v}_h\cdot\mathbf{n}_e)\,\mathrm{d}\gamma \\ \qquad - \displaystyle\sum_{e\in\xi_h^{\mathrm{N}}}\frac{1}{\alpha}\int_e (g_{\mathrm{N}})(\mathbf{v}_h\cdot\mathbf{n}_e)\,\mathrm{d}\gamma \\ \qquad - \displaystyle\sum_{e\in\xi_h'}\frac{1}{2\alpha}\int_e [\![-K\nabla p_h\cdot\mathbf{n}_e]\!][\![\mathbf{v}_h\cdot\mathbf{n}_e]\!]\,\mathrm{d}\gamma, \end{cases} \tag{31}$$

where $-K\nabla p_h$ denotes the Darcy velocity calculated element-wise by simple differentiation.

This problem is well posed. In fact, we have the following result:

Proposition 3 *Let p_h be a computed approximation of the solution $p \in H^s(\tau_h), s \geq 2$ of Eq. 1 satisfying the estimations (11). There exists a unique solution $\mathbf{u}_h$ of problem (31). Moreover, if $\mathbf{u} = -K\nabla p$ and $\alpha = \frac{\sigma k^2}{h}$, then there exists a constant C independent of h and k such that*

$$\sum_{E\in\tau_h} \|\mathbf{u}-\mathbf{u}_h\|^2_{0,E} \leq C\frac{h^{2\mu-2}}{k^{2s-3}}\left(\sum_{E\in\tau_h}\|\mathbf{u}\|^2_{s,E}+\sum_{E\in\tau_h}\|p\|^2_{s,E}\right), \tag{32}$$

$$\sum_{e\in\xi_h'} \|[\![(\mathbf{u}-\mathbf{u}_h)\cdot\mathbf{n}_e]\!]\|^2_{0,e} + \sum_{e\in\xi_h^{\mathrm{N}}} \|(\mathbf{u}-\mathbf{u}_h)\cdot\mathbf{n}_e\|^2_{0,e} \leq C\frac{h^{2\mu-3}}{k^{2s-5}}\left(\sum_{E\in\tau_h}\|\mathbf{u}\|^2_{s,E}+\sum_{E\in\tau_h}\|p\|^2_{s,E}\right), \tag{33}$$

where $\mu = \min(k+1, s)$.

Proof See Appendix 2. □

Remark 2

– The Darcy velocity can now be recovered by the inversion of a block-diagonal matrix. This is a local-

in-the-cell process, which reduces the computational efforts.
– Because in Eq. 31 there is no interface stability term in the left-hand side, the penalty parameter α will undergo specific constraint; see Eq. 34, for the right-hand-side term $[\![-K\nabla p_h]\!]$ not to pollute the recovered velocity.

4.2.1 Estimation of the stability parameter

We address in this section the dependence of the penalty parameter α with respect to the stability parameter β. We claim here that there is a specific relationship between the penalty parameter α, in the problem (31), and the stability parameter β in Eq. 12. More precisely the following holds:

Proposition 4 *Let p_h be the approximate solution of Eq. 1 satisfying Eq. 11 and β the parameter in Eq. 12. Let α be the penalty parameter in formulation (31).*

If there exists a constant $\sigma_0 > 0$ sufficiently large such that

$$\alpha \geq \sigma_0 \beta, \tag{34}$$

then there exists a constant $C > 0$ independent of β such that

$$\sum_{E\in\tau_h}\int_E K^{-1}\mathbf{u}_h\cdot\mathbf{u}_h\,\mathrm{d}x+\sum_{e\in\xi_h^{'}}\frac{1}{\alpha}\int_e[\![\mathbf{u}_h\cdot\mathbf{n}_e]\!]^2\,\mathrm{d}\gamma$$
$$+\sum_{e\in\xi_h^{\mathrm{N}}}\frac{1}{\alpha}\int_e(\mathbf{u}_h\cdot\mathbf{n}_e)^2\,\mathrm{d}\gamma\leq CC^*(f,P_{\mathrm{D}},g_{\mathrm{N}}). \tag{35}$$

Proof See Appendix 6. □

Remark 3 We can refine the determination of parameter σ_0 as follows:

Define

$$\kappa=\max_{E\in\tau_h}\frac{(k+1)(k+d)}{4\lambda_m^E d}\frac{|\partial E|}{|E|},$$

with λ_m^E and d given in Section 2 by formula (3). If the parameter β in Eq. 12 is selected in a way that there exists a constant $\varpi > 0$ such that

$$\frac{3\beta}{4\kappa}-\frac{1}{\varpi}>0\qquad\text{then}\qquad\sigma_0\geq\frac{1}{\sqrt{\frac{3\beta}{4\kappa}-\frac{1}{\varpi}}}. \tag{36}$$

For practical considerations, it is sufficient to take $\alpha \geq \beta$.

4.3 Third velocity reconstruction approach

The remark above states that in the previous reconstruction (Eq. 31), the penalty parameter has to be chosen carefully so that the jumps of the normal derivatives of the primal variable do not disturb the recovered velocity. As an alternative, we now consider a particular strategy which consists in splitting the penalty terms in Eq. 27 while maintaining the recovery process elementwise. The problem now reads

$$\begin{cases}\text{Find } \mathbf{u}_h\in\Sigma_h^k \quad\text{such that } \forall\mathbf{v}_h\in\Sigma_h^k,\quad \forall E\in\tau_h,\\ \displaystyle\int_E K^{-1}\mathbf{u}_h\cdot\mathbf{v}_h\,\mathrm{d}x+\frac{1}{2\alpha}\int_{\partial E\cap\partial E'}\mathbf{u}_h\cdot\mathbf{n}\,\mathbf{v}_h\cdot\mathbf{n}\,\mathrm{d}\gamma\\ \quad+\displaystyle\frac{1}{\alpha}\int_{\partial E\cap\Gamma_{\mathrm{N}}}\mathbf{u}_h\cdot\mathbf{n}\,\mathbf{v}_h\cdot\mathbf{n}\,\mathrm{d}\gamma\\ \quad=-\displaystyle\int_E\nabla p_h\cdot\mathbf{v}_h\,\mathrm{d}x\\ \quad\quad-\displaystyle\frac{1}{2\alpha}\int_{\partial E\cap\partial E'}(K'\nabla p_h')\cdot\mathbf{n}\,\mathbf{v}_h\cdot\mathbf{n}\,\mathrm{d}\gamma\\ \quad\quad+\displaystyle\frac{1}{2}\int_{\partial E\cap\partial E'}(p_h-p_h')\mathbf{v}_h\cdot\mathbf{n}\,\mathrm{d}\gamma\\ \quad\quad+\displaystyle\int_{\partial E\cap\Gamma_{\mathrm{D}}}(p_h-p_{\mathrm{D}})\,\mathbf{v}_h\cdot\mathbf{n}\,\mathrm{d}\gamma\\ \quad\quad-\displaystyle\frac{1}{\alpha}\int_{\partial E\cap\Gamma_{\mathrm{N}}}g_{\mathrm{N}}\,\mathbf{v}_h\cdot\mathbf{n}\,\mathrm{d}\gamma,\end{cases} \tag{37}$$

We can show the following:

Proposition 5 *Let p_h be a computed approximation of the solution $p\in H^s(\tau_h), s\geq 2$ of Eq. 1 satisfying the estimations (11). There exists a unique solution u_h of problem (37). Moreover, if $\mathbf{u}=-K\nabla p$ and $\alpha=\frac{\sigma k^2}{h}$, then there is a constant C independent of h and k such that*

$$\sum_{E\in\tau_h}\|\mathbf{u}-\mathbf{u}_h\|_{0,E}^2$$
$$\leq C\frac{h^{2\mu-2}}{k^{2s-3}}\left(\sum_{E\in\tau_h}\|\mathbf{u}\|_{s,E}^2+\sum_{E\in\tau_h}\|p\|_{s,E}^2\right), \tag{38}$$

$$\sum_{e\in\xi_h^{'}}\|[\![(\mathbf{u}-\mathbf{u}_h)\cdot\mathbf{n}_e]\!]\|_{0,e}^2+\sum_{e\in\xi_h^{\mathrm{N}}}\|(\mathbf{u}-\mathbf{u}_h)\cdot\mathbf{n}_e\|_{0,e}^2$$
$$\leq C\frac{h^{2\mu-3}}{k^{2s-5}}\left(\sum_{E\in\tau_h}\|\mathbf{u}\|_{s,E}^2+\sum_{E\in\tau_h}\|p\|_{s,E}^2\right), \tag{39}$$

where $\mu=\min(k+1,s)$.

Proof See Appendix 3. □

4.3.1 Estimation of the stability parameter

We address in this section the potential dependence of the penalty parameter α with respect to the stability parameter β. We claim here that there is no relationship between the penalty parameter α, in the problem (37), and the stability parameter β in Eq. 12. More precisely the following result holds:

Proposition 6 *Let p_h be the approximate solution of Eq. 1 satisfying Eq. 11 and β the parameter in Eq. 12. For any penalty parameter α in formulation (37), there exists a constant $C > 0$ independent of β such that*

$$\sum_{E\in\tau_h}\int_E K^{-1}\mathbf{u}_h\cdot\mathbf{u}_h\,\mathrm{d}x+\sum_{e\in\xi_h'}\frac{1}{\alpha}\int_e[\![\mathbf{u}_h\cdot\mathbf{n}_e]\!]^2\,\mathrm{d}\gamma$$
$$+\sum_{e\in\xi_h^{\mathrm{N}}}\frac{1}{\alpha}\int_e(\mathbf{u}_h\cdot\mathbf{n}_e)^2\,\mathrm{d}\gamma\le CC^*(f,P_{\mathrm{D}},g_{\mathrm{N}}).\qquad(40)$$

Proof See Appendix 7. □

5 Numerical illustration

In this sub-section, we carry out a numerical test to compare the Darcy velocity obtained in four manners from the solution of the primal formulation (20).

The first is the simple local differentiation which consists in determining $\mathbf{u}_h$ in each element $E\in\tau_h$ by the formula $\mathbf{u}_h=-K\nabla p_h$. It is favorable to write it in the form

$$\int_E K^{-1}\mathbf{u}_h\cdot\mathbf{v}_h\,\mathrm{d}x$$
$$=-\int_E\nabla p_h\cdot\mathbf{v}_h\,\mathrm{d}x,\forall\mathbf{v}_h\in\mathcal{P}_k(E).\qquad(41)$$

The second manner is given by Eq. 31, the third by Eq. 27, and the fourth by Eq. 37.

We first start by the convergence error in L^2 and in L^∞ norms of the normal jump. This is done in Section 5.1 and will validate the fact that each approximation gives reasonable result as far as high-order polynomial is used and the velocity remains smooth. In Section 5.2, we carry out a comparison test which will make evident the differences among all the mentioned reconstructions. This comparison is based on a graphical criterion: If we represent graphically a velocity in each cell of the mesh by plotting the vector of the velocity at each vertex of the cell, each vertex of the mesh will receive as vector as the total number of the cell containing that vertex. Consequently, for an affine velocity, unless the approximated velocity is well constructed, the represented vectors at each vertex will not coincide. This is a well-defined criterion to check whether a good global affine approximation of the velocity is obtained. This section is closed in Section 5.4 by showing that whatever the velocity reconstruction, a better computation of the pressure is required, unless one may face specific difficulties notably on boundary conditions of Dirichlet type.

5.1 Numerical evaluation of the error estimate

To illustrate the numerical convergence, we consider the test case with smooth solution as given in [7]. Consider $\Omega=(0,1)^2$, $\Gamma_{\mathrm{N}}=\emptyset$. The permeability tensor K is isotropic and constant, with value 1. We choose the boundary conditions and the right-hand side such that the exact solution of Eq. 1 is $p=e^{-\left((x-\frac{1}{2})^2+(y-\frac{1}{2})^2\right)}$. We then compute the pressure p by formula (20) using different polynomial orders and the Darcy velocity with formulae (41), (27), (31), and (37) using the same polynomial order and the same stability parameter, i.e., $\alpha=\frac{\sigma}{h}$ with $\sigma=100$. We then compute the L^2 error between the exact velocity and the velocity obtained by the different reconstructions. The L^2 error on the normal component of the velocity is also computed as $\max_{e\in\xi_h'}\|[\![\mathbf{u}_h\cdot\mathbf{n}_e]\!]\|_{0,e}$. To evaluate the convergence rate, we start with a uniform mesh of the domain made of $2\times8\times8$ triangles and successively apply a dyadic refinement of the mesh. We compute the rate for any error e_h by the formula $\ln\left(e_h/e_{\frac{h}{2}}\right)/\ln(2)$, where h is the mesh size. The results for polynomials of orders 1, 2, and 3 are reported in Tables 1 and 2.

We observe that all the reconstructions provide the same convergence rate, and no differences are observed when higher-order polynomials are used. In our test case, this occurs when polynomial of orders 2 and 3 are used. To better observe the differences between the above-mentioned reconstructions, we need a specific test case. This is the aim of Section 5.2.

5.2 Comparison of the different approaches

While building the above-mentioned velocity reconstructions, we aimed at the continuity of the normal component along the interfaces between cells. Hence, to better compare the provided reconstructions, we now base our analysis on a graphical criterion. As the Darcy velocity is approximated by totally discontinuous

Table 1 Numerical L^2 errors and convergence rate associated, for the different velocity reconstructions with first ($\mathcal{P}_1$)-, second ($\mathcal{P}_2$)-, and third ($\mathcal{P}_3$)-order polynomials, with parameters $\alpha = \frac{\sigma}{h}, \sigma = 100$

h^{-1}	Formulation (41)		Formulation (27)		Formulation (31)		Formulation (37)	
	Error	Rate	Error	Rate	Error	Rate	Error	Rate
	$\mathcal{P}_1$							
8	7.598e−02	–	7.148e−02	–	7.121e−02	–	7.135e−02	–
16	3.802e−02	1.00	3.576e−02	1.00	3.562e−02	1.00	3.570e−02	1.00
32	1.901e−02	1.00	1.788e−02	1.00	1.781e−02	1.00	1.785e−02	1.00
64	9.507e−03	1.00	8.943e−03	1.00	8.908e−03	1.00	8.926e−03	1.00
128	4.753e−03	1.00	4.471e−03	1.00	4.454e−03	1.00	4.463e−03	1.00
	$\mathcal{P}_2$							
8	2.545e−03	–	2.249e−03	–	2.238e−03	–	2.257e−03	–
16	6.388e−04	1.99	5.645e−04	1.99	5.620e−04	1.99	5.670e−04	1.99
32	1.599e−04	2.00	1.414e−04	2.00	1.408e−04	2.00	1.420e−04	2.00
64	4.000e−05	2.00	3.537e−05	2.00	3.522e−05	2.00	3.555e−05	2.00
128	1.000e−05	2.00	8.847e−06	2.00	8.807e−06	2.00	8.891e−06	2.00
	$\mathcal{P}_3$							
8	9.344e−05	–	8.423e−05	–	8.280e−05	–	8.368e−05	–
16	1.167e−05	3.00	1.053e−05	3.00	1.035e−05	3.00	1.046e−05	3.00
32	1.458e−06	3.00	1.317e−06	3.00	1.293e−06	3.00	1.307e−06	3.00
64	1.822e−07	3.00	1.646e−07	3.00	1.616e−07	3.00	1.634e−07	3.00
128	2.278e−08	3.00	2.257e−08	2.87	2.020e−08	3.00	2.043e−08	3.00

polynomials, we represent for each triangle, the local velocity vector at its middle edges. Therefore, on an internal edge, two vectors are displayed. For the test carried out, these two vectors should coincide. Indeed, the test will be selected so that the exact velocity is linear on a part of the domain and almost null on the rest of the domain.

To better observe the differences between the three approaches, we start with a pressure (p_h) obtained by a first-order approximation for which a simple local differentiation would give a constant velocity in each element. We then plot the magnitude of the velocity obtained by each reconstruction. Our comparison criterion is based of the fact that if the velocity is piecewise constant, the representation will show a piecewise constant color in each cell.

We now specify the test carried out. Consider $\bar{\Omega} = \bar{\Omega}_1 \cup \bar{\Omega}_2$, with $\Omega_1 = (-1, 0) \times (-1, 1)$ and $\Omega_2 = (0, 1) \times (-1, 1)$. The permeability tensor K is isotropic and constant in Ω_1 and Ω_2 where these constants are $K_1 = 1$ and $K_2 = 10^{-4}$, respectively. Let us choose the boundary conditions and the right-hand side function such that $p(x, y) = x^2 + y^2$ is the exact solution. The domain is equipped with a uniform grid made of $2 \times 10 \times 10$ triangles. On each edge e, we take $\alpha = \sigma/|e|$ with $\sigma = 10$. We take first-order polynomials to approximate the

Table 2 Numerical evaluation of $\max_{e \in \xi_h'} \|[\![\mathbf{u}_h \cdot \mathbf{n}_e]\!]\|_{0,e}$ and its convergence rate for the different velocity constructions, for first ($\mathcal{P}_1$)-, second ($\mathcal{P}_2$)-, and third ($\mathcal{P}_3$)-order polynomials, with parameters $\alpha = \frac{\sigma}{h}, \sigma = 100$

h^{-1}	Formulation (41)		Formulation (27)		Formulation (31)		Formulation (37)	
	Error	Rate	Error	Rate	Error	Rate	Error	Rate
	$\mathcal{P}_1$							
8	8.504e−02	–	8.023e−02	–	7.994e−02	–	8.009e−02	–
16	3.048e−02	1.48	2.876e−02	1.48	2.865e−02	1.48	2.871e−02	1.48
32	1.082e−02	1.49	1.020e−02	1.49	1.017e−02	1.49	1.019e−02	1.49
64	3.827e−03	1.50	3.611e−03	1.50	3.598e−03	1.50	3.604e−03	1.50
128	1.353e−03	1.50	1.277e−03	1.50	1.272e−03	1.50	1.274e−03	1.50
	$\mathcal{P}_2$							
8	1.610e−03	–	1.227e−03	–	1.188e−03	–	1.205e−03	–
16	2.925e−04	2.46	2.150e−04	2.51	2.068e−04	2.52	2.107e−04	2.52
32	5.260e−05	2.48	3.837e−05	2.49	3.681e−05	2.49	3.759e−05	2.49
64	9.380e−06	2.49	6.858e−06	2.48	6.582e−06	2.48	6.719e−06	2.48
128	1.666e−06	2.49	1.219e−06	2.49	1.171e−06	2.49	1.195e−06	2.49
	$\mathcal{P}_3$							
8	1.499e−04	–	1.264e−04	–	1.212e−04	–	1.241e−04	–
16	1.355e−05	3.47	1.142e−05	3.47	1.096e−05	3.47	1.121e−05	3.47
32	1.204e−06	3.49	1.015e−06	3.49	9.741e−07	3.49	9.968e−07	3.49
64	1.066e−07	3.50	8.988e−08	3.50	8.622e−08	3.50	8.823e−08	3.50
128	9.424e−09	3.50	7.97e−09	3.50	7.623e−09	3.50	7.801e−09	3.50

pressure using Eq. 20 and construct the Darcy velocity by each of the four above-mentioned approaches.

Figure 1 displays the computed velocity fields. It represents graphically the velocity vectors in the middle edge of each element. Namely, two vectors are drawn at the middle point of each internal edge of the mesh, each from inside the adjacent elements. In an affine approximation of the velocity, these two vectors must coincide.

Observations

1. For this test case, the three suggested reconstructions are better than the simple local differentiation, in the sense that the angles between the vectors on an internal edge are smaller and their modules are less different.
2. At any interface, the normal component of the velocity obtained by the second reconstruction is less continuous than the one obtained by the first reconstruction.
3. One notes from Fig. 2, which represents the magnitude of the velocity, that the third construction approaches much more simple construction, while providing a velocity which is almost element-wise linear. It represents a better $\mathcal{P}_1$ reconstruction.
4. If the stability parameter is selected too large, the various reconstructions provide an almost identical

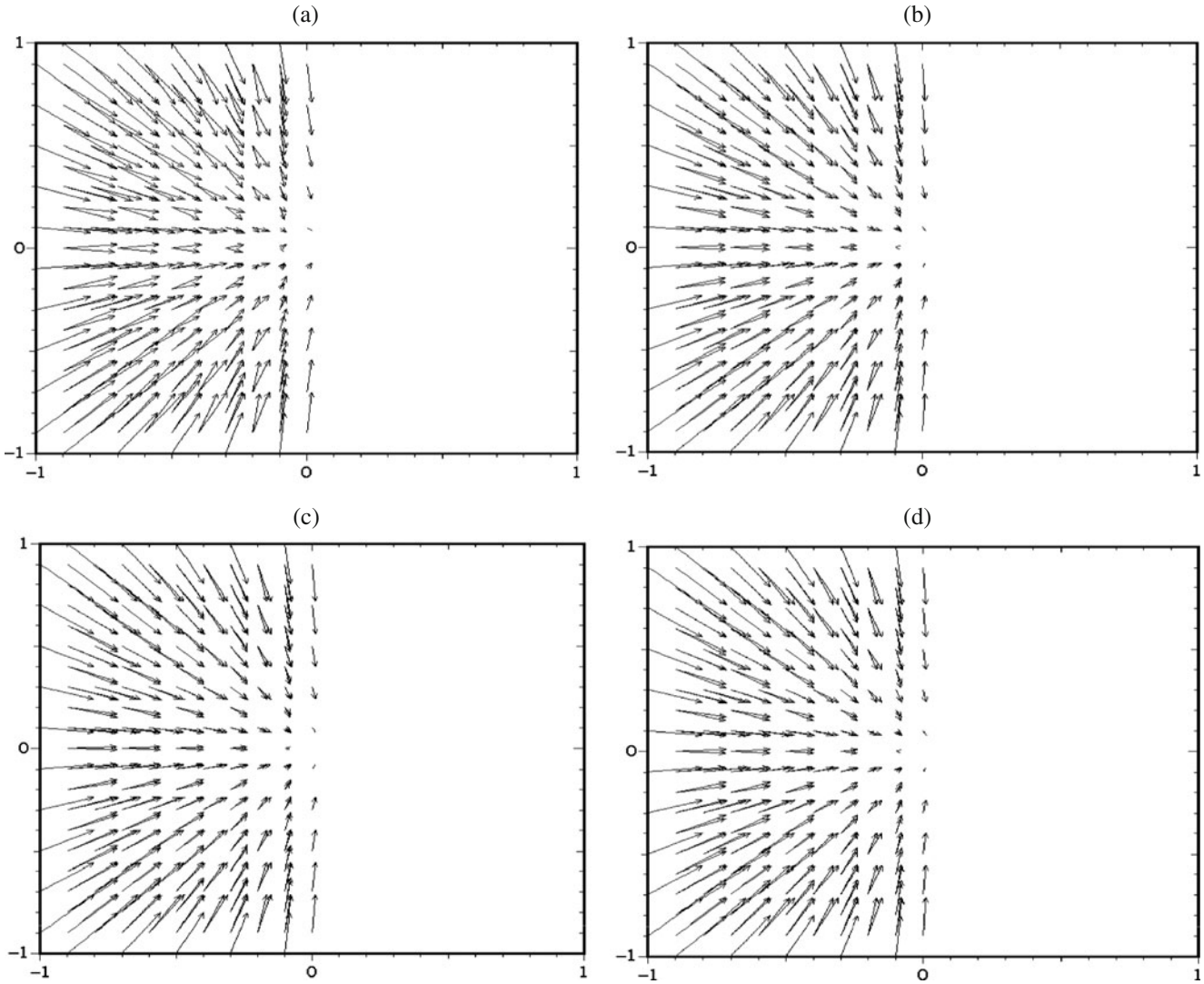

Fig. 1 Darcy's velocity built from $\mathcal{P}_1$ pressure approximation with a permeability ratio $\frac{K_1}{K_2} = 10^{-4}$. The fields are obtained by graphically drawing the Darcy velocity vector in the middle edges of each element. **a** Field for simple differentiation reconstruction (Eq. 41). **b** Field for first reconstruction (Eq. 27). **c** Field for second reconstruction (Eq. 31). **d** Field for third reconstruction (Eq. 37)

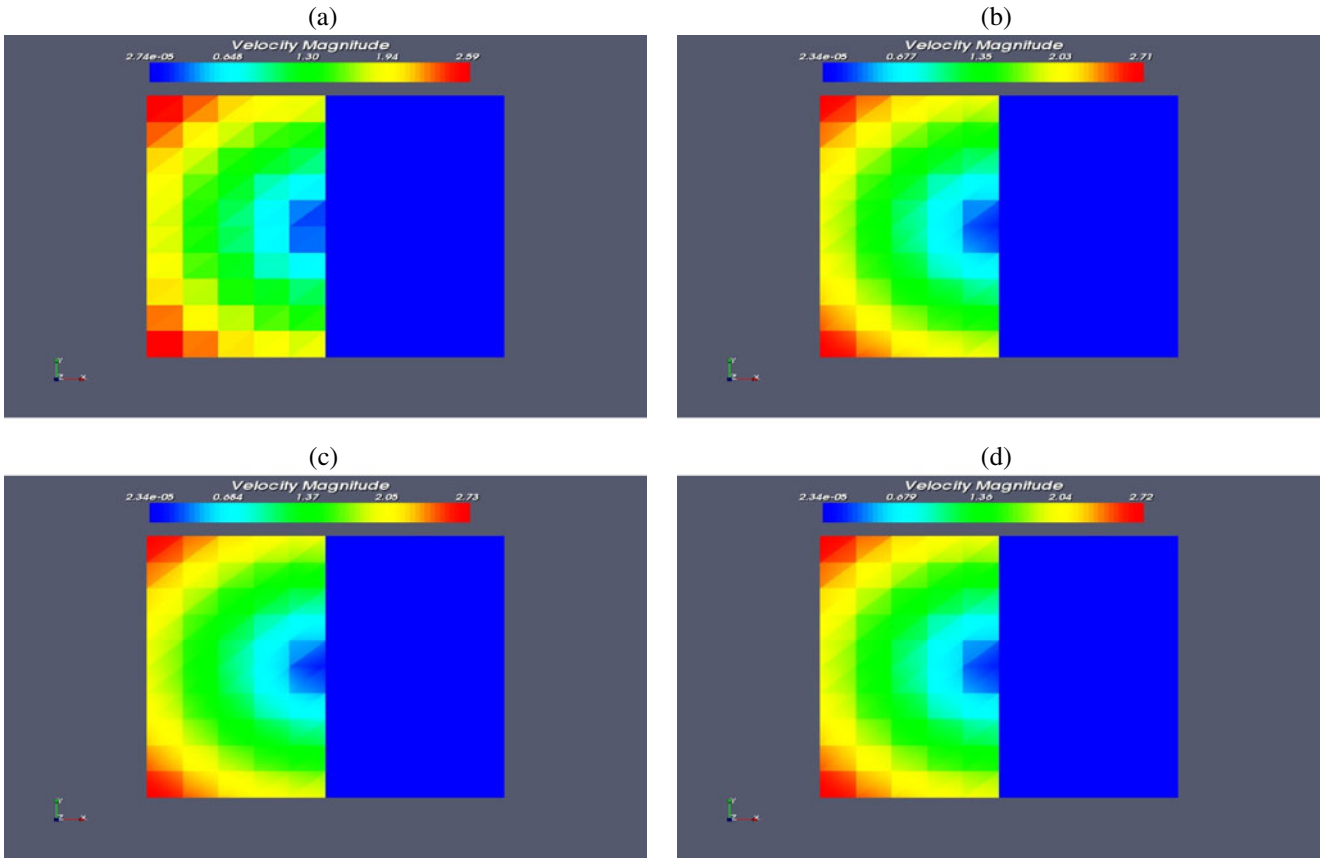

Fig. 2 $\mathcal{P}_1$—the magnitude of the Darcy velocity built from $\mathcal{P}_1$ pressure approximation, for a permeability ratio of $\frac{K_1}{K_2} = 10^{-4}$. **a** Magnitude for simple reconstruction (Eq. 41); **b** magnitude for reconstruction (Eq. 27); **c** magnitude for reconstruction (Eq. 31); **d** magnitude for reconstruction (Eq. 37)

result. Because in this case, the continuity of the solution at the interfaces between elements is reinforced, making the approximation "almost" conformal. We know that in such an approximation, the degree of the polynomial for approximating the velocity must be one unit lower than that of the pressure.

5. If the stabilization makes the primal problem almost conformal, a better reconstruction strategy is either to increase the order of the polynomial approximation or to resort to post-processing using other finite element types, when these are applicable (see [7, 19]). However, the first reconstruction of the velocity can be viewed as a penalty, with jumps, of the simple local differentiation; the penalty parameter can therefore be different from that used to solve the primal formulation. Consequently, the penalty parameter can be adjusted in formulation (27) in order to recover the velocity with a more continuous normal component at the interface between elements. As an illustration, let us run once more the previous test case with a penalty parameter ten times smaller on internal edges of the triangles. The graphical output is shown in Fig. 3. It can be observed that the continuity of the Darcy velocity at the interfaces between cells is better. Since the exact velocity is affine over the domain Ω, it also appears that the reconstructed velocity is a better affine approximation of the exact velocity.

5.3 The penalty parameter adjusted in formulation (27)

In this subsection, we numerically show that the convergence rate of the method is not destroyed by adjusting the penalty parameter when the Darcy velocity is derived by formulation (27). We have already seen that this can improve the continuity of the normal component of the velocity. By running again the previous graphical test case with a more smaller penalty parameter α in Eq. 27, we observe in Fig. 3 that a better continuity of the normal component of the velocity at interfaces between cells is achieved.

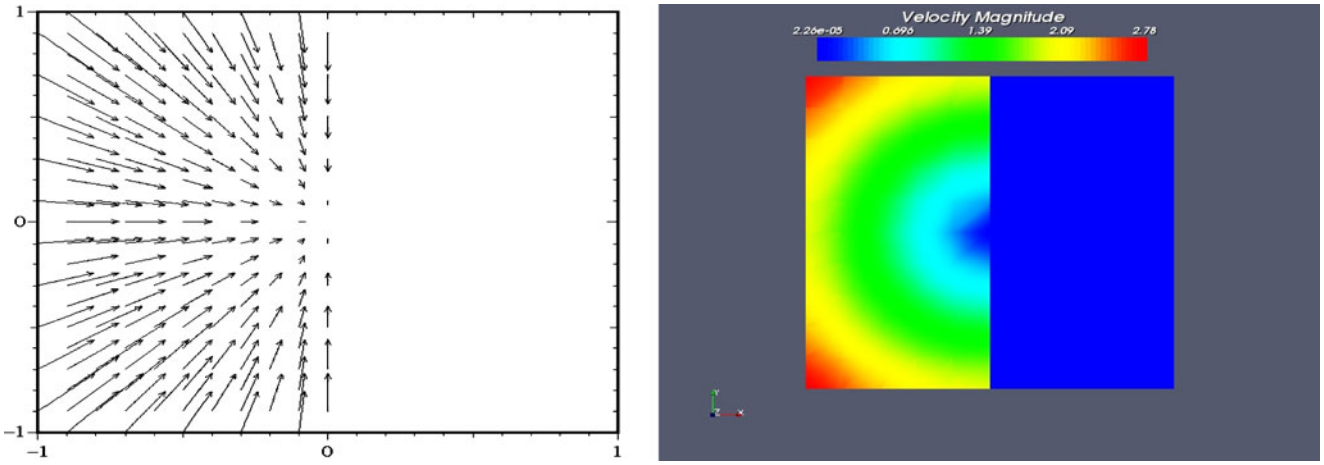

Fig. 3 The field (*left*) and the magnitude (*right*) of the Darcy velocity for reconstruction (Eq. 27) with $\sigma = 10$ on Dirichlet edges and $\sigma = 1/10$ on internal edges, obtained by a $\mathcal{P}_1$ approximation of pressure using Eq. 20 with a permeability ratio $\frac{K_1}{K_2} = 10^{-4}$ and $\sigma = 10$ on all edges. The velocity field is represented by drawing a vector on the middle edge of any element, from inside that element

We also carry out the convergence test case of the previous subsection, Section 5.2. The pressure is still obtained from Eq. 20 with a stability parameter taken to be $\beta_h = \sigma \frac{k^2}{h}$ with $\sigma = 10$. But the velocity is now computed by using Eq. 27 with an adjusted penalty parameter α_h. Namely, $\alpha_h = \sigma \frac{k^2}{h}$ with $\sigma = 10$ on boundary faces and $\sigma = 1/10$ on internal faces. The results are displayed in Table 3. Although the convergence rate is almost identical to that of Table 2, the error is smaller. More precisely we make the following observations:

- For first-order polynomials, the convergence rate in L^2 norm now starts at $\frac{3}{2}$ instead of 1 previously obtained and decreases to 1 very slowly as the mesh is refined. Also, the error in the jump of the normal component of the velocity is 75 times smaller. Consequently, this method is suited for coarse meshes and low-order polynomials. These are exactly the situations where the global nature of the reconstruction is not too costly.
- Concerning polynomials of order 2, although the convergence rate is the same, the error in L^2 norm is twice smaller and the error in the jump of the normal component is 50 times smaller.
- With polynomials of order 3, the same order of convergence is observed. However, the error in L^2 norm is 1.5 times smaller, and the error in the jump of the normal components of the velocity is 150 times smaller.

Unfortunately there is no general criterion for quantifying the gain when the penalty parameter is adjusted. The conclusion drawn is that the penalty parameter adjustment in formulation (27) can improve substantially the error on the jumps of the normal components of the velocity.

Table 3 Numerical L^2 errors and $\max_{e\in\xi_h'} \|[\![\mathbf{u}_h \cdot \mathbf{n}_e]\!]\|_{0,e}$ and convergence rates associated with reconstruction (27) when the penalty parameter $\alpha_h = \sigma \frac{k^2}{h}$ with $\sigma = 10$ on boundary edges and $\sigma = 1/10$ on internal edges and first ($\mathcal{P}_1$)-, second ($\mathcal{P}_2$)-, and third ($\mathcal{P}_3$)-order polynomials are used

h^{-1}	$\mathcal{P}_1$		$\mathcal{P}_2$		$\mathcal{P}_3$	
	Error	Rate	Error	Rate	Error	Rate
	$\|\mathbf{u} - \mathbf{u}_h\|_{0,\Omega}$					
8	7.997e−03	–	1.274e−03	–	5.698e−05	–
16	2.528e−03	1.66	3.157e−04	2.01	7.091e−06	3.01
32	8.489e−04	1.57	7.869e−05	2.00	8.849e−07	3.00
64	3.027e−04	1.49	1.965e−05	2.00	1.105e−07	3.00
128	1.148e−04	1.40	4.910e−06	2.00	1.406e−08	2.97
	$\max_{e\in\xi_h'} \|[\![u_h \cdot \mathbf{n}_e]\!]\|_{0,e}$					
8	1.197e−03	–	2.796e−05	–	8.583e−07	–
16	4.273e−04	1.49	5.057e−06	2.47	7.727e−08	3.47
32	1.514e−04	1.50	9.013e−07	2.49	6.861e−09	3.49
64	5.357e−05	1.50	1.598e−07	2.50	6.072e−10	3.50
128	1.894e−05	1.50	2.829e−08	2.50	5.436e−11	3.48

5.4 The impact of the approximation of the pressure

In this section, we would like to highlight one important issue which is the impact of the poor pressure approximation in the post-processing of the Darcy velocity. We claim that if the boundary condition is not well enforced when solving the pressure equation, this may lead to an oscillation of the computed velocity in the cells connected to that part of the boundary.

To make this asset more evident, let us consider problem (1) with constant permeability $K(x, y) = 1$ a Dirichlet boundary condition on the whole boundary of $\Omega =]0, 1[\times]0, 1[$. The right-hand side and the boundary condition are such that the exact solution is $p(x, y) = x^2 + y^2$. With a locally refine quadrilateral mesh around the bottom left corner $(0, 0)$, we compute the pressure by the same primal DG formulation (20) but with different penalty parameter when enforcing the Dirichlet boundary condition: For the first one, we take $\beta_h = 10/h$, and for the second one, we take $\beta_h = 100/h$. Then for each of the computed pressure, we compute the velocity using formulation (27) with the same penalty parameter ($\alpha_h = 10^{-4}/h$). The results are displayed in Fig. 4.

Since the expected velocity over the domain is $\mathbf{v}(x, y) = (-2x, -2y)$, we can draw the following conclusion: Even though the poor approximation of the pressure p_h might not affect the normal component of the computed velocity, it considerably affect the value of the velocity inside cells. Luckily, the affected ones are only boundary cells closed to the Dirichlet boundary where the pressure was badly approximated. Consequently, the error due to bad approximation of the pressure at the boundary of a particular cell does not propagate outside that cell as far as the global property of the velocity is concerned, such as global constancy or global linearity.

6 Comparison with other post-processing

In this section, we perform more numerical tests to compare the proposed reconstructions with available post-processing methods. We start situating our approaches into family of DG method in Section 6.1. We then compare our approaches to projection into conformal spaces in Section 6.2. We conclude by

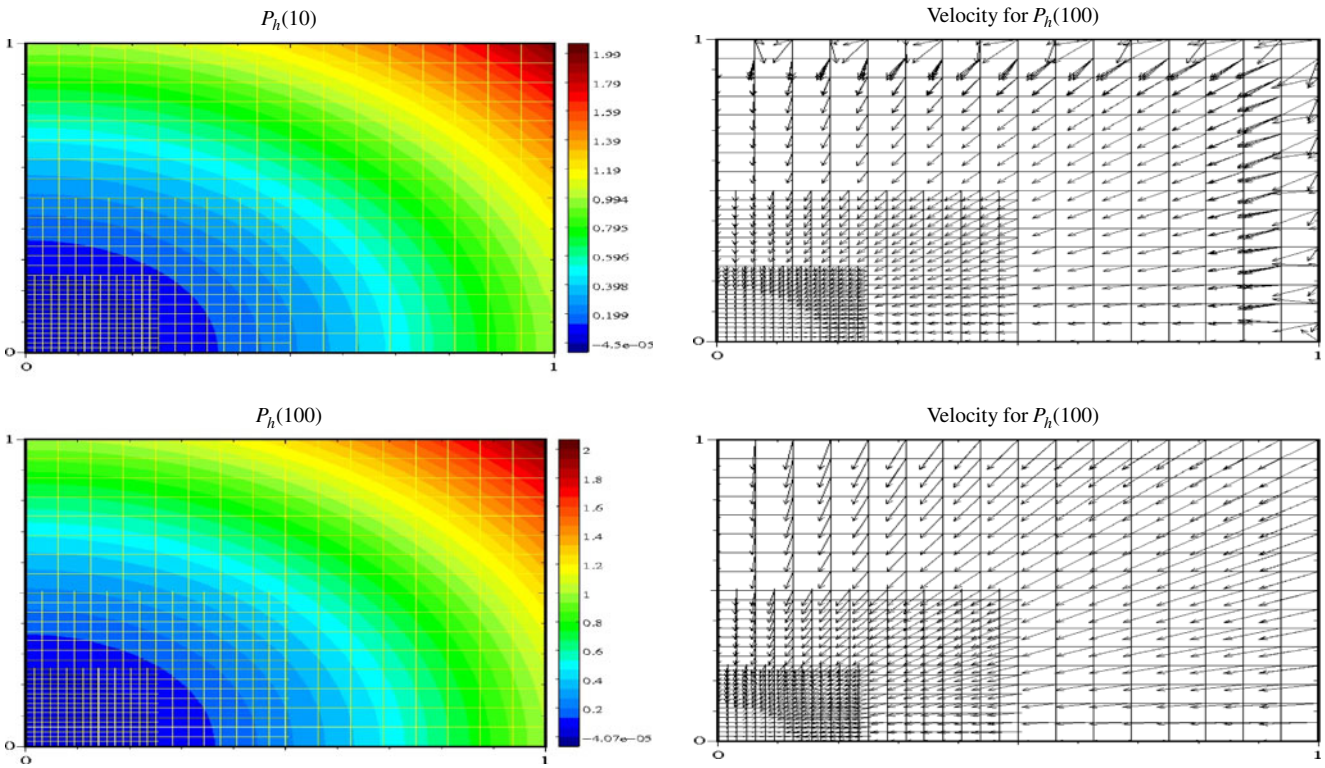

Fig. 4 $\mathcal{P}_1$ Darcy velocity for two different origins of pressure: first line $\mathcal{P}_1$ pressure with Dirichlet penalty parameter $\sigma = 10$ (denoted $P_h(10)$). Second line $\mathcal{P}_1$ pressure with Dirichlet penalty parameter $\sigma = 100$ (denoted $P_h(100)$). The pressure is obtained using DG formulation from Eq. 20. The plot of the velocity is obtained by drawing one vector at each vertex of each element, from inside that element

evaluating our approaches on general meshes and a non-isotropic problem in Section 6.3.

6.1 Connection with other discontinuous Galerkin methods

The formulations (27) and (37), at a first sight, look like available post-processing techniques in the mixed DG formulation. However, this is not the case and consequently ensures the novelty of our proposed post-processing. Let us highlight it in more details.

For the sake of simplicity, we assume here that $K = I$, and consequently, the velocity needed to be approximated is $\mathbf{u} = -\nabla p$. In the DG theory, see for instance [4, 23], the equation for defining the velocity is formulated as: seek $\mathbf{u}_h \in \Sigma_h^k$ such that for all $\mathbf{v}_h \in \Sigma_h^k$

$$\int_\Omega \mathbf{u}_h \cdot \mathbf{v}_h \,\mathrm{d}x = \int_\Omega p_h(\nabla \cdot \mathbf{v}_h)\,\mathrm{d}x - \sum_{E\in\tau_h} \int_{\partial E} \hat{p}_E(\mathbf{v}_h \cdot \mathbf{n}_E)\,\mathrm{d}\gamma, \tag{42}$$

where $\hat{p}$ is the pressure flux to be defined appropriately. Various choices are available as listed in Table 4 below (see [4] for more details).

As it is straightforward, none of these methods proposes the penalty approach for computing the velocity. On contrary, each of our proposed methods, namely Eqs. 27, 31, and 37, proposes a penalty approach. This can be seen by rearranging terms in each of them, which results on internal edges only to the Table 5.

However, as we have pointed out, the quality of the approximation of the pressure is important. The LDG method and most mixed DG method achieve this good quality approximation of the pressure by instead working on the complementary equation associated to Eq. 42 (see references [4, 23] for more details). Since our formulations work well whatever the origin of the pressure, the pressure from LDG formulation will only be beneficial and will keep us from the problem mentioned in Section 5.4.

Table 4 Various selections of $\hat{p}$ in the discontinuous Galerkin methods

Method	$\hat{p}_E$ on $e = \partial E \cap \partial E'$
Bassi–Rebay	$\{p_h\}$
Brezzi et al. 1	$\{p_h\}$
LDG	$\{p_h\} - (\gamma \cdot \mathbf{n}_E)[\![p_h]\!]$
IP	$\{p_h\}$
Bassi et al.	$\{p_h\}$
Baumann–Oden	$\{p_h\} + [\![p_h]\!]$
NIPG	$\{p_h\} + [\![p_h]\!]$
Babuska–Zlamal	$(p_h\|_E)\|_{\partial E}$
Brezzi et al. 2	$(p_h\|_E)\|_{\partial E}$

As reviewed in [4]. The jump is from internal to external

Table 5 Analog value for $\hat{p}$ in our penalty formulation, with E' the neighboring cell of E, $\mathbf{n}_E$ is the outward unit normal at the boundary of E and the jump is from inside to outside of the element E

Method	$\hat{p}_E$ on $e = \partial E \cap \partial E'$
First (Eq. 27)	$\{p_h\} + \frac{1}{\alpha}[\![\mathbf{u}_h]\!] \cdot \mathbf{n}_E$
Second (Eq. 31)	$\{p_h\} - \frac{1}{\alpha}[\![\nabla p_h]\!] \cdot \mathbf{n}_E$
Third (Eq. 37)	$\{p_h\} + \frac{1}{\alpha}\left((\mathbf{u}_h\|_E) + (\nabla p_h\|_{E'})\right)\|_{\partial E} \cdot \mathbf{n}_E$

6.2 Comparison against some projections into conformal spaces

We are aware of two conformal $H(\mathrm{div})$ projections, namely the local projection into the BDM space [7] and the projection into the Raviart Thomas (RT) space [19]. We are also aware of the Zienkiewicz and Zhu projection [32]. This projection is known to be optimal. But its purpose is to construct a velocity such that each component falls in the conformal Lagrange finite element on the given mesh, with better approximated nodal values. This is achieved by introducing specific macro-element around each nodal point and careful selections of interpolation points (quadrature points) for the least squares problem. Although this method gives a good result at nodal points, is not constructed in view of achieving the continuity of the normal component of the velocity. We are not aware of its extension to general distorted meshes, with dangling nodes. Its implementation is not straightforward because the selection of the interpolation points for the least squares problem is not obvious for high-order polynomials (see [32]). For these reasons, we have not implemented the method, but we advocate that it will be interesting to see how it can be extended on general meshes and how it behaves on full anisotropic permeability tensor.

Because BDM and RT spaces are related to conformal approximation, their extension to general meshes is either not straightforward or almost impossible in general. Consequently, in this sequel, we will consider only triangular meshes. We refer to [7, 19] for the detailed definition of these projections; however, we remind that attention should be paid at the implementation level as highlighted below.

In all the numerical experiments presented in this section, on contrary to [19], where it is advised to use the exact flux from the primal formulation, we make the choice, as in [7] to use the mean value of the velocity

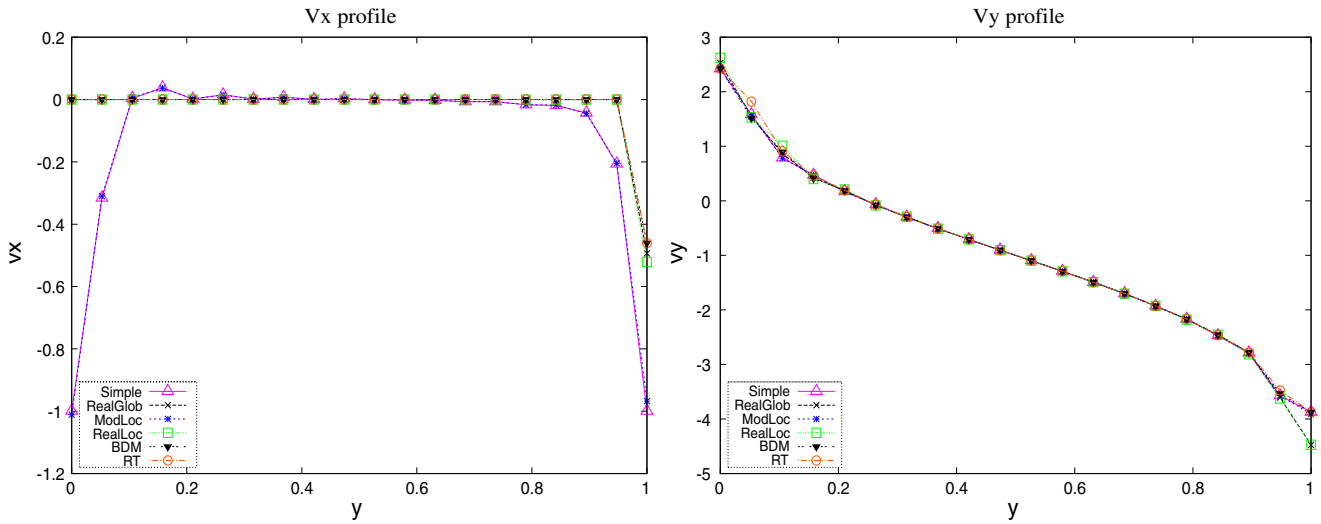

Fig. 5 Profile of the velocities along the line $x = 0.5$, for the test case of Section 6.2.1. On the *left* the first component, on the *right* the second component

obtained by direct differentiation. Consequently, we will define these projections as follows: Let $\mathbf{u}^{DG}$ be the DG velocity obtained by direct differentiation in each cell of the mesh. The projection of [7] which we will denote BDM is defined on each element E with edges $e_i, i = 1, 2, 3$, by Eq. 43, while the projection of [19], which we will denote RT, is given by Eq. 44

$$\begin{cases} \text{Find } \mathbf{u}^* \in (\mathcal{P}_{k-1}(E))^2 : \\ \int_{e_i} \left(\mathbf{u}^* - \{\mathbf{u}^{\mathrm{DG}}\}\right) \cdot \mathbf{n}_{e_i} w \, \mathrm{d}\gamma = 0, \ \forall w \in \mathcal{P}_{k-1}(e_i), \\ \int_E \left(\mathbf{u}^* - \mathbf{u}^{\mathrm{DG}}\right) \cdot \nabla w \, \mathrm{d}x \quad = 0, \ \forall w \in \mathcal{P}_{k-2}(E), \\ \int_E \left(\mathbf{u}^* - \mathbf{u}^{\mathrm{DG}}\right) \cdot \mathbf{S}(w) \, \mathrm{d}x \quad = 0, \ \forall w \in \mathcal{M}_k(E). \end{cases} \tag{43}$$

where $\mathbf{S}(w) = (\frac{\partial w}{\partial y}, -\frac{\partial w}{\partial x})$ and $\mathcal{M}_k(E)$ is the space of polynomials vanishing on the boundary of E

$$\mathcal{M}_k(E) = \{v \in \mathcal{P}_k(E) : v|_{\partial E} = 0\} \equiv \lambda_1\lambda_2\lambda_3\mathcal{P}_{k-3}(E),$$

where λ_i, $i = 1, 2, 3$ are the barycentric coordinates.

$$\begin{cases} \text{Find } \mathbf{u}^* \in \mathrm{RT}_{k-1}(E) : \\ \int_{e_i} \left(\mathbf{u}^* - \{\mathbf{u}^{\mathrm{DG}}\}\right) \cdot \mathbf{n}_{e_i} w \, \mathrm{d}\gamma = 0, \ \forall w \in \mathcal{P}_{k-1}(e_i), \\ \int_E \left(\mathbf{u}^* - \mathbf{u}^{\mathrm{DG}}\right) \cdot \mathbf{w} \, \mathrm{d}x \quad = 0, \ \forall \mathbf{w} \in (\mathcal{P}_{k-2}(E))^2 . \end{cases} \tag{44}$$

where $\mathrm{RT}_k(E) = \mathcal{P}_k^2(E) \oplus (x, y)\mathcal{P}_k(E)$.

Let us point out some difficulties that make the implementation not so easy:

- In Eq. 43, the space $\mathcal{P}_{k-2}(E)$ should be understood as $\mathcal{P}_{k-2}(E) \setminus \mathcal{P}_0(E)$.
- In Eq. 44, some implementation tricks are needed to fulfill the direct sum: $\mathrm{RT}_k(E) = \mathcal{P}_k^2(E) \oplus (x, y)\mathcal{P}_k(E)$.

All this make the implementation of the projection not only straightforward but also complicated or almost

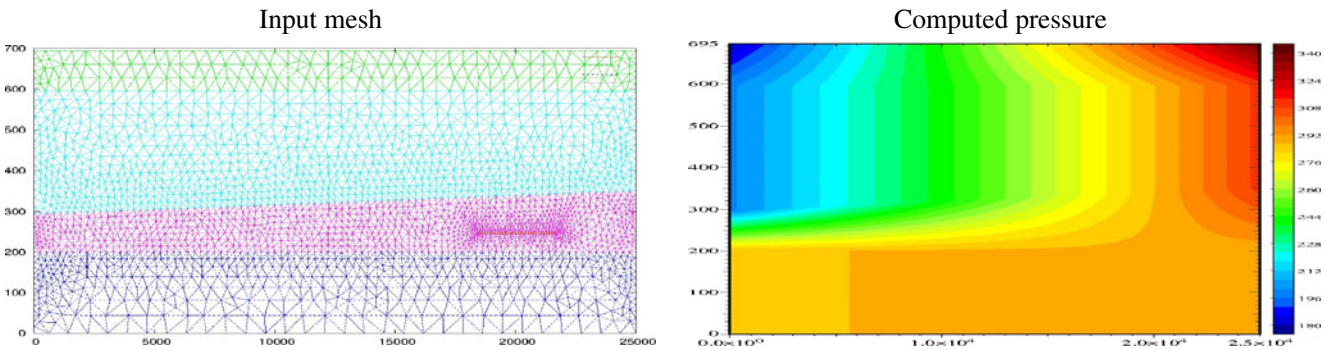

Fig. 6 Mesh and the pressure solution for the Couplex I problem

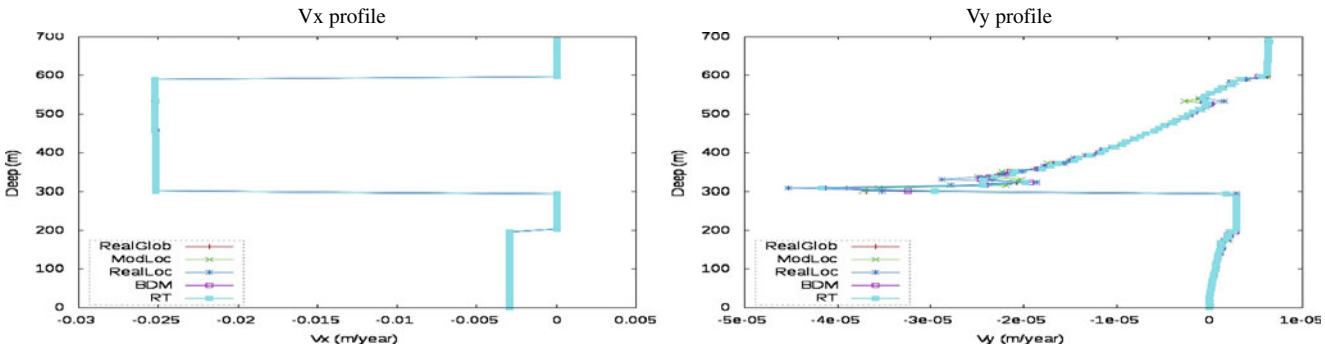

Fig. 7 Profiles of the velocity along the vertical line $x = 50$ for the Couplex I problem, using various post-processing

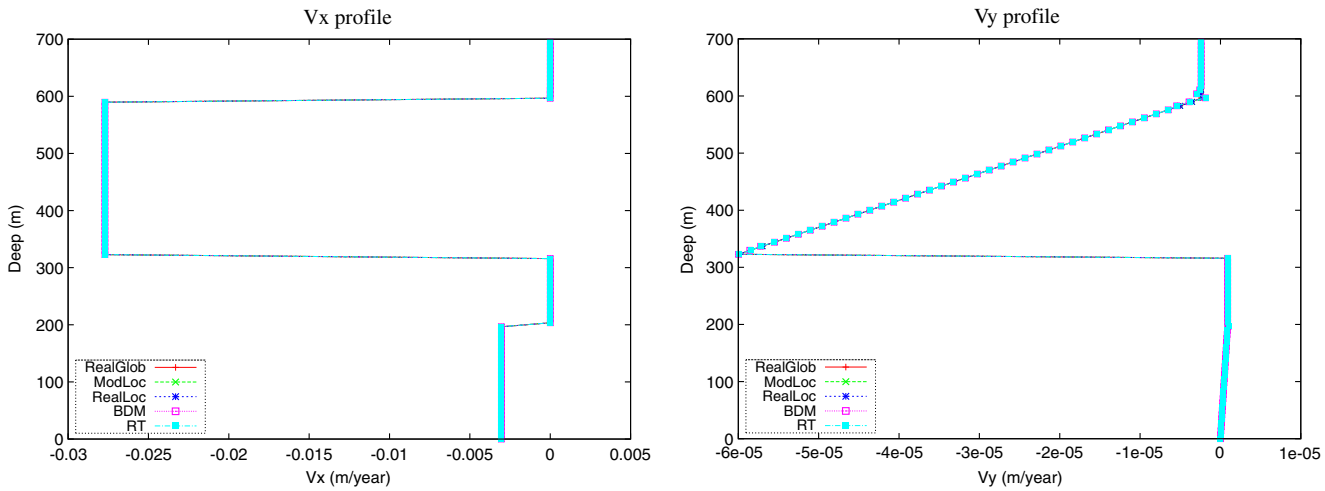

Fig. 8 Profiles of the velocity along the vertical line $x = 12{,}500$ for the Couplex I problem, using various post-processing

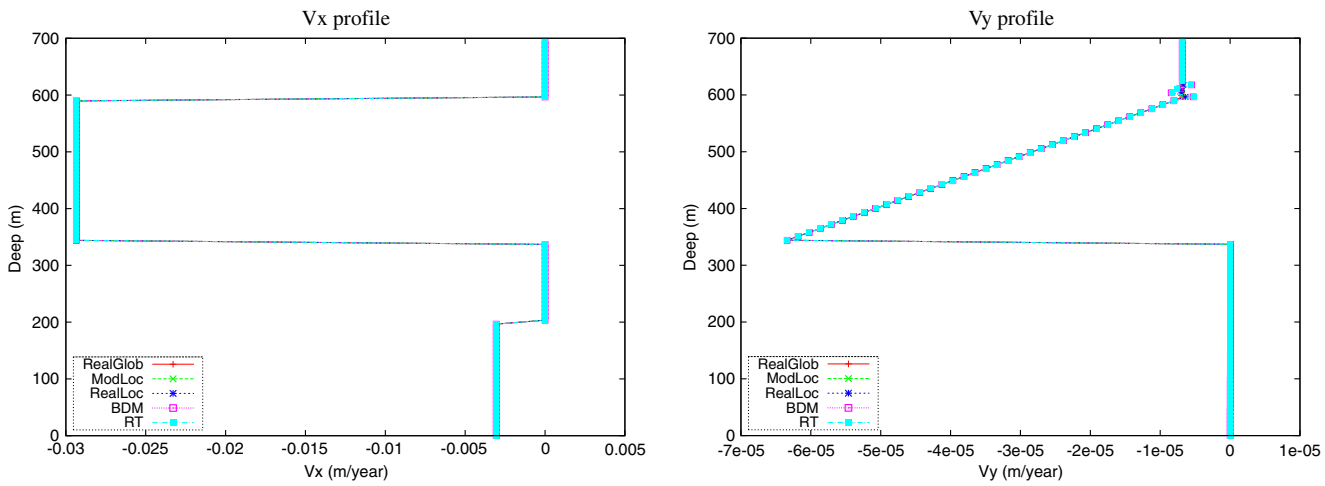

Fig. 9 Profiles of the velocity along the vertical line $x = 20{,}000$ for the Couplex I problem, using various post-processing

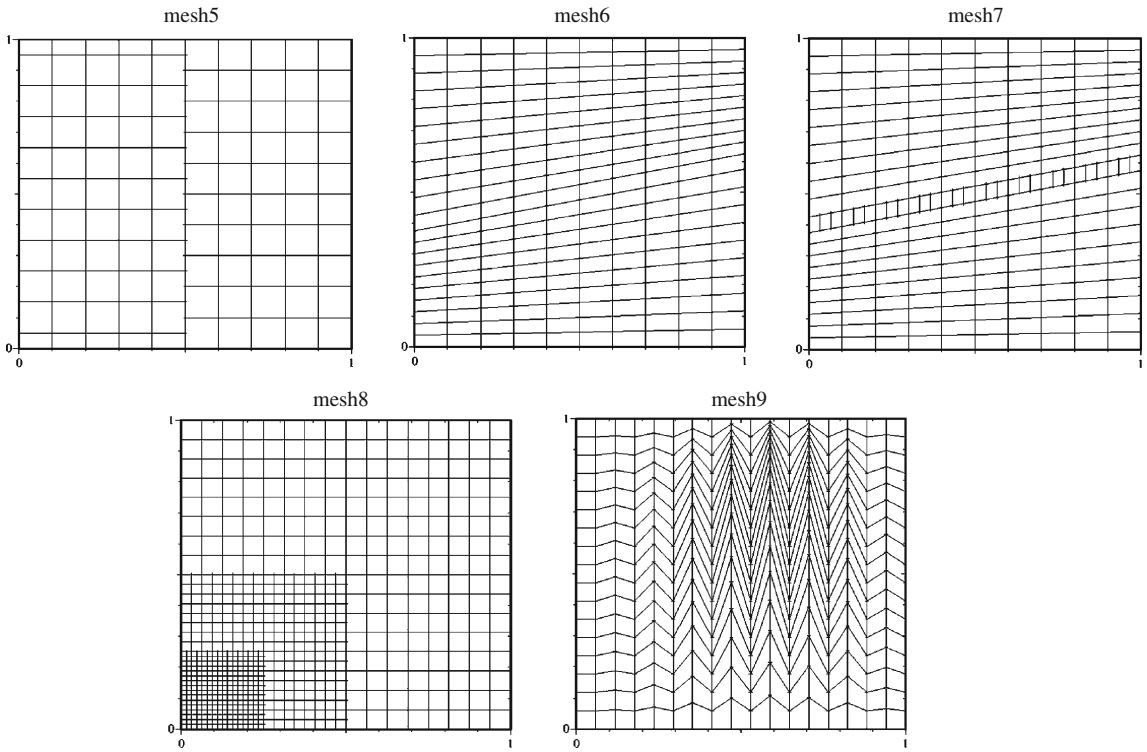

Fig. 10 Input meshes for testing the behavior of Darcy velocity post-processing

impossible on general distorted meshes with dangling nodes. Let us also point out that Raviart Thomas space is unstable on distorted meshes see [24].

However, these projections are advised when working with conformal meshes. They are highly recommended. But because their extensions to non-

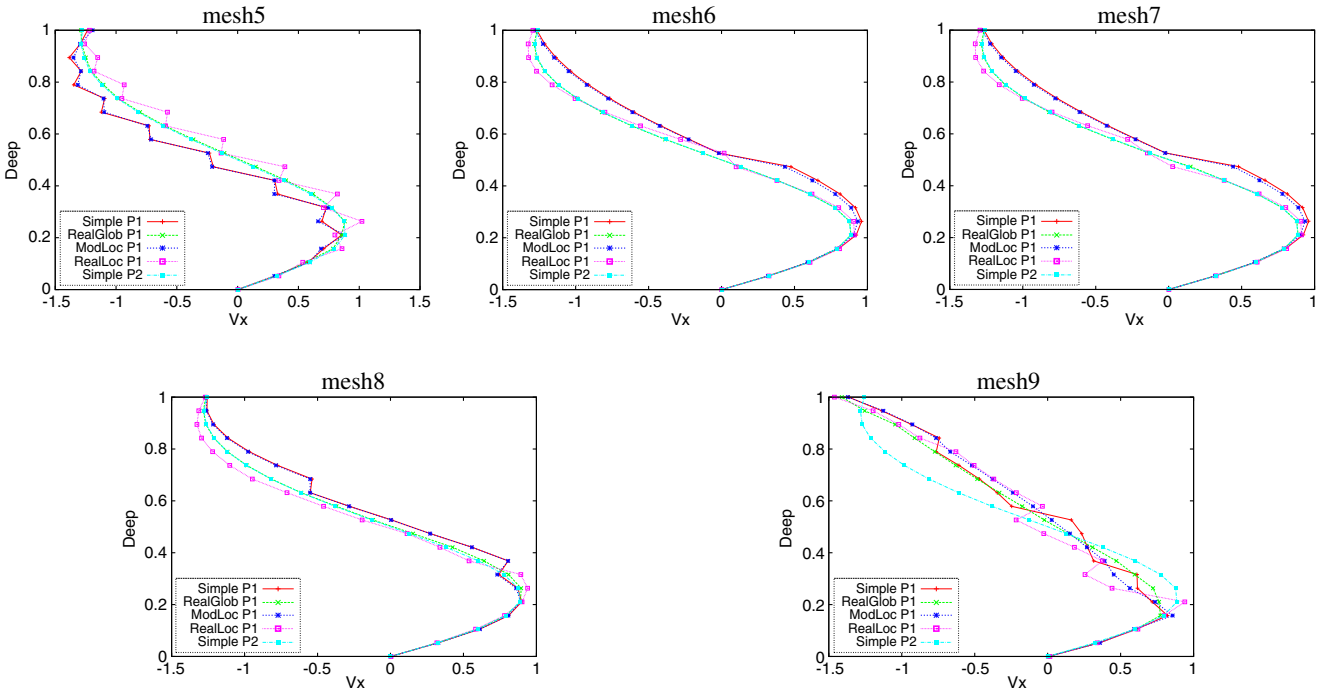

Fig. 11 Profile of the horizontal component of the computed velocity on 20 equally distributed points on the vertical line $x = 0.5$. The solution using P2 polynomial and direct differentiation is displayed for comparison

Table 6 L2-norm and jump of the normal component of the velocity for various reconstructions, using P1 polynomials

The pressure is computed using also P1 polynomials

Mesh5	mesh6	mesh7	mesh8	mesh9	
$\max_{e\in\xi_h'} \|[\![\mathbf{u}_h \cdot \mathbf{n}_e]\!]\|_{0,e}$					
1.897e−01	1.330e−01	1.330e−01	9.606e−02	5.805e−01	Simple
5.703e−03	7.093e−03	7.094e−03	5.641e−04	6.269e−03	RealGlob
3.113e−01	1.918e−01	1.918e−01	1.019e−01	3.617e−01	ModLoc
1.654e−01	1.081e−01	1.081e−01	8.173e−02	5.687e−01	RealLoc
$\|\mathbf{u} - \mathbf{u}_h\|_{0,\Omega}$					
1.449e−01	1.139e−01	1.134e−01	8.047e−02	3.810e−01	Simple
1.559e−01	1.091e−01	1.083e−01	1.111e−02	2.363e−01	RealGlob
1.856e−01	1.362e−01	1.349e−01	7.841e−02	3.170e−01	ModLoc
1.279e−01	7.634e−02	7.494e−02	5.419e−02	3.508e−01	RealLoc

conformal meshes are not straightforward, the penalty approaches presented in the present paper are welcome. The penalty approaches are not only comparable to conformal projection on conformal meshes but they apply also on non-conformal and distorted meshes, as shown in Sections 6.2.1 and 6.2.2,

6.2.1 Comparison on a simple domain Ω

We consider the test case of Section 5.2, but now with $\Omega_1 = (0, 0.5) \times (0, 1)$ and $\Omega_2 = (0.5, 1) \times (0, 1)$. The pressure is computed using symmetric version of Eq. 20, with stability parameter $\beta_h = \sigma/|e|$ with $\sigma = 180$ and second-order polynomials. The velocity is then computed using formula 41 named here (Simple), Eq. 27 named here (RealGlob), Eq. 31 named here (ModLoc), Eq. 37 named here (RealLoc), formula (43) named here (BDM), and Eq. 44 named here (RT). The penalty parameter is taken $\alpha_h = \beta_h/100$ except for Eq. 31 where $\alpha_h = \beta_h$.

We compute the profile of the velocity along the line $x = 0.5$ with 20 equally distant points. We display the x-coordinate and the y-coordinate of the velocity on Fig. 5. We see that for these selections of parameters, all the reconstructions are at worst equivalent to the direct differentiation, while all of our proposed reconstructions, except the Eq. 31, are comparable to local $H(\mathrm{div})$ projections. Note that because the parameter in the primal formulation is selected large $\beta_h = \sigma/|e|$ with

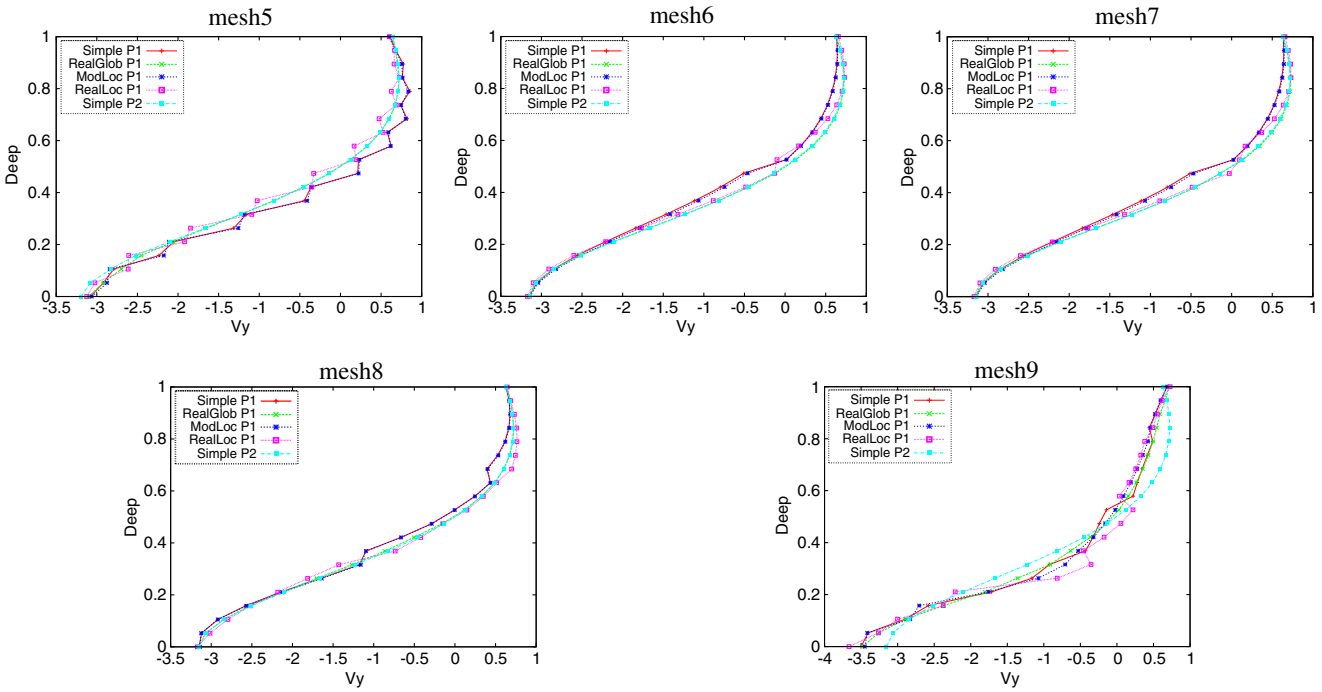

Fig. 12 Profile of the vertical component of the computed velocity on 20 equally distributed points on the vertical line $x = 0.5$. The solution using P2 polynomial and direct differentiation is displayed for comparison

$\sigma = 180$, the constraint Eq. 34 brings the formulation (31) close to Eq. 41 which explains the similar behavior in Fig. 5.

6.2.2 Comparison on a more complicated domain Ω

In this section, we consider the hydrodynamic problem of Couplex I (see [6, 8]). For the input mesh, see Fig. 6; the mesh size is $h = 1{,}005.36$ m. We compute the pressure using our formulation 20, with third-order polynomial, and stability parameter $\beta_h = \sigma/|e|$, with $\sigma = 100 \times 1005.36 \times 4$. The result is displayed in Fig. 6.

The velocity is then post-processed as above. The penalty parameter is selected as follows: For formulation 31, we take $\alpha_h = \beta_h$, while for the others, we take $\alpha_h = \beta_h \times 10^{-7}$.

The profiles of the first and second components of the velocity along three vertical lines are displayed in Figs. 7, 8, and 9. We observe some small oscillations on the right picture of Fig. 7, which disappear as the polynomial order grows. It might be due to the approximation of the pressure. However, these computations show for this difficult problem a comparative behavior of our formulation with local projection into conformal $H(\mathrm{div})$ spaces.

6.3 Evaluation on distorted meshes with anisotropic tensors

Let us now observe the behavior of the proposed reconstructions for an anisotropic problem over a domain equipped with distorted and not necessary conformal meshes. These situations can occur in porous media because of the tectonic movement of soil. These are sample problems for which the application of local $H(\mathrm{div})$ projection like those described above are, to

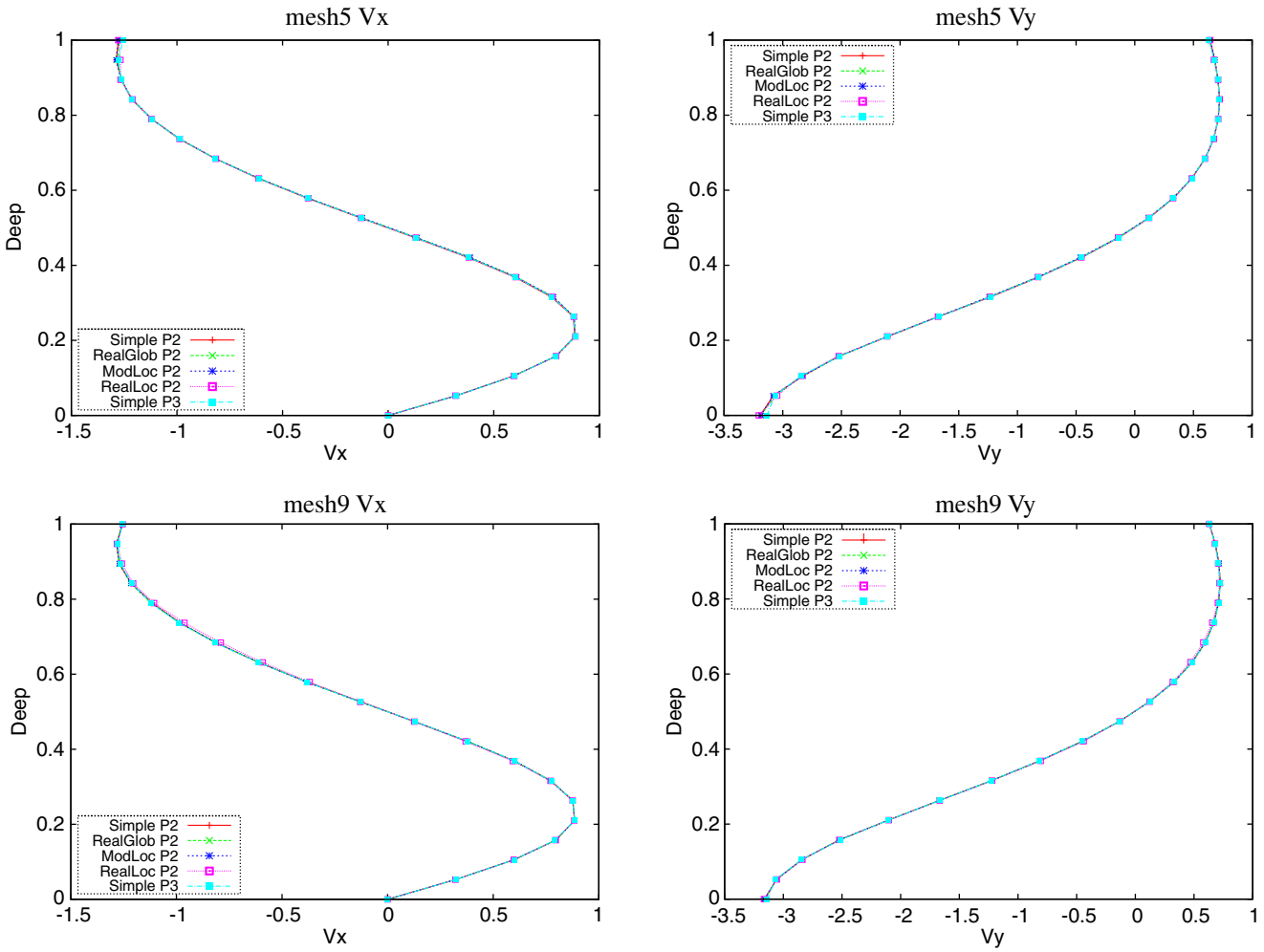

Fig. 13 Profile of the computed velocity on 20 equally distributed points on the vertical line $x = 0.5$. The solution using P3 polynomial and the direct differentiation is displayed for comparison

our knowledge, either not straightforward or impossible. Recall that the BDMk or RTk spaces require a conformal meshes, which need not be distorted (see the explanation in [24]). This is why in this section, we only consider the reconstructions presented in this paper, namely RealGlob (see Eq. 27), ModLoc (see Eq. 31), and RealLoc (see Eq. 37) and occasionally the direct differentiation (see Eq. 41 identified as (Simple)).

The considered domain Ω is meshed as depicted in Fig. 10. The permeability tensor is given in each case. The boundary condition is only of Dirichlet, when the exact solution is supply the right-hand side and the boundary conditions are obtained from the exact solution. The permeability tensor is given by

$$K(x,y)=\frac{1}{(x^2+y^2)}\begin{pmatrix}\varepsilon x^2+y^2 & (\varepsilon-1)xy\\ (\varepsilon-1)xy & x^2+\varepsilon y^2\end{pmatrix}, \tag{45}$$

with $\varepsilon=10^{-3}$. The right-hand side and the Dirichlet boundary condition are obtained from the exact solution $p(x,y)=\sin(\pi x)\sin(\pi y)$. This problem is known to induce numerical locking for some schemes.

The pressure is once again computed using formulation 20, with parameter $\beta_h=100/|e|$, and the velocity is obtained as above with parameter $\alpha_h=\beta_h\times 10^{-4}$ except for the constrained reconstruction where we take $\alpha_h=\beta_h$. As Fig. 11 shows, it is better to stay on first-order polynomials to observe the differences. Hence, we use only first-order polynomials (quadratic in this sequel), and for all the meshes, we display in Table 6 the jump of the normal component of the velocity and the error in L2-norm on the computed velocity. We also display in Figs. 12 and 13 the profile of the velocity on the vertical line passing in the middle of the domain.

As it is clearly apparent, the reconstruction (RealGlob), i.e., Eq. 27, is the best among the proposed reconstructions, with only first-order polynomial; the result is close to direct differentiation of second-order polynomial. The second best reconstruction for the consider problem is (RealLoc), i.e., Eq. 37; it is the one which furnishes solutions which are the closest to Eq. 27. As before, reconstruction (Eq. 31) is more close to direct differentiation because of the penalty parameter constraint here.

7 Conclusion

We have provided three techniques for computing the Darcy velocity: Eqs. 27, 31, and 37. They are particular stabilizations of the simple local-to-one-cell differentiation technique but designed to perform better in unfavorable cases of large computing where the computer resources do not allow for high-order polynomial approximations. All methods are shown to ensure optimal convergence order. Moreover, we have made the following observations, depending on whether the main concern is efficiency or memory limitation:

1. Formulation (27) is the best in accuracy, since its stabilization parameter can be adjusted to obtain better Darcy velocity. However, it is rather memory consuming because it does not provide decoupled block diagonal matrix. It is advisable to use this formulation when the size of the problem is not too large. It is of great interest when using parallel distributed memory programming.
2. Unlike formulation (27), formulation (31) provides a block diagonal matrix, which ensures local-in-the-cell computation of the Darcy velocity. It provides the best result for certain stability parameters. Unfortunately, the determination of this particular stability parameter is not available. Its specific feature is that it requires to be above a threshold stability parameter, whose value is provided (see Eq. 36).
3. The third reconstruction (Eq. 37) lies in between the two above-mentioned reconstructions and shares the properties of both. It provides a block-diagonal matrix as does Eq. 31 and exhibits no constraint on the stability parameter as does Eq. 27. We highly recommend this formulation if the size of the problem is big or should be adjusted dynamically.

Beside this, all the presented velocity reconstructions are designed completely decoupled from the pressure equations because they are specific penalty of the continuous lifting operator at the discrete level. However, here like in general reconstructions, a poor pressure approximation can deteriorate the post-processed Darcy velocity.

Acknowledgements The author's research was supported by a grant from the research group MoMaS (Mathematical Modeling and Numerical Simulation for Nuclear Waste Management Problems).

Appendix 1: Proof of Proposition 1

Proof of Proposition 1 Let

$$\mathcal{G}(\mathbf{u},\mathbf{v})=\sum_{E\in\tau_h}\int_E K^{-1}\mathbf{u}\mathbf{v}\,\mathrm{d}x+\sum_{e\in\xi_h'}\frac{1}{2\alpha}\int_e[\![\mathbf{u}\cdot\mathbf{n}_e]\!][\![\mathbf{v}\cdot\mathbf{n}_e]\!]\,\mathrm{d}\gamma$$
$$+\sum_{e\in\xi_h^{\mathrm{N}}}\frac{1}{\alpha}\int_e(\mathbf{u}\cdot\mathbf{n}_e)(\mathbf{v}\cdot\mathbf{n}_e)\,\mathrm{d}\gamma, \tag{46}$$

$$\mathcal{F}(p;\mathbf{v}) = -\sum_{E\in\tau_h}\int_E \mathbf{v}\cdot\nabla p\,\mathrm{d}x + \sum_{e\in\xi_h'}[\![p]\!]\{\mathbf{v}\cdot\mathbf{n}_e\}\,\mathrm{d}\gamma + \sum_{e\in\xi_h^{\mathrm{D}}} p(\mathbf{v}\cdot\mathbf{n}_e)\,\mathrm{d}\gamma. \tag{47}$$

Existence and uniqueness of the discrete velocity The space Σ_h^k is of finite dimension. Hence, it suffices to show the uniqueness of the solution. Let $\mathbf{v}\in\Sigma_h^k$ be such that $\mathcal{G}(\mathbf{v},\mathbf{v})=0$. Therefore, $\sum_{E\in\tau_h}\int_E (K^{-1}\mathbf{v})\cdot\mathbf{v}\,\mathrm{d}x = 0$. Since K is elliptic, so does K^{-1}. Consequently, $||v||_{0,E}^2 = 0\ \forall\ E\in\tau_h$ and $v\equiv 0$.

Error estimates Denote $\eta=\mathbf{u}-\hat{\mathbf{u}}$ and $\zeta=\hat{\mathbf{u}}-\mathbf{u}_h$, where $\hat{\mathbf{u}}$ is an interpolation of $\mathbf{u}$ satisfying for each component the relation (10) given by the Lemma 2. We have

$$\begin{aligned}\mathcal{G}(\zeta,\zeta) &= -\mathcal{G}(\eta,\zeta)+\mathcal{G}(\mathbf{u},\zeta)-\mathcal{G}(\mathbf{u}_h,\zeta)\\ &= -\mathcal{G}(\eta,\zeta)-\mathcal{F}(p-p_h;\zeta),\end{aligned} \tag{48}$$

which implies

$$|\mathcal{G}(\zeta,\zeta)| \le |\mathcal{G}(\eta,\zeta)| + |\mathcal{F}(p-p_h;\zeta)|. \tag{49}$$

Therefore, applying the triangular inequality, we get

$$\begin{aligned}|\mathcal{G}(\eta,\zeta)| &\le A_1+A_2+A_3,\\ |\mathcal{F}(p-p_h;\zeta)| &\le L_1+L_2+L_3,\end{aligned} \tag{50}$$

where $A_i, L_i, i=1,2,3$ are given below. Using the algebraic inequality $ab\le \epsilon a^2+\frac{1}{4\epsilon}b^2$, which is true for any real numbers a, b, and $\epsilon>0$, they are bounded as follows:

$$\begin{aligned}A_1 &= \sum_{E\in\tau_h}\int_E |(K^{-1}\eta)\cdot\zeta|\,\mathrm{d}x \le c_1\sum_{E\in\tau_h}\|\eta\|_{0,E}\|\zeta\|_{0,E}\\ &\le c_1\epsilon_1\sum_{E\in\tau_h}\|\zeta\|_{0,E}^2 + \frac{c_1}{4\epsilon_1}\sum_{E\in\tau_h}\|\eta\|_{0,E}^2,\end{aligned} \tag{51}$$

$$\begin{aligned}A_2 &= \sum_{e\in\xi_h'}\frac{1}{2\alpha}\int_e |[\![\eta\cdot\mathbf{n}_e]\!][\![\zeta\cdot\mathbf{n}_e]\!]|\,\mathrm{d}\gamma\\ &\le \epsilon_2\sum_{e\in\xi_h'}\frac{1}{2\alpha}\|[\![\zeta\cdot\mathbf{n}_e]\!]\|_{0,e}^2 + \frac{1}{4\epsilon_2}\sum_{e\in\xi_h'}\frac{1}{2\alpha}\|[\![\eta\cdot\mathbf{n}_e]\!]\|_{0,e}^2,\end{aligned} \tag{52}$$

$$\begin{aligned}A_3 &= \sum_{e\in\xi_h^{\mathrm{N}}}\frac{1}{\alpha}\int_e |(\eta\cdot\mathbf{n}_e)(\zeta\cdot\mathbf{n}_e)|\,\mathrm{d}\gamma\\ &\le \epsilon_3\sum_{e\in\xi_h^{\mathrm{N}}}\frac{1}{\alpha}\|(\zeta\cdot\mathbf{n}_e)\|_{0,e}^2 + \frac{1}{4\epsilon_3}\sum_{e\in\xi_h^{\mathrm{N}}}\frac{1}{\alpha}\|(\eta\cdot\mathbf{n}_e)\|_{0,e}^2,\end{aligned} \tag{53}$$

$$\begin{aligned}L_1 &= \sum_{E\in\tau_h}\int_E |\zeta\cdot\nabla(p-p_h)|\,\mathrm{d}x\\ &\le \epsilon_4\sum_{E\in\tau_h}\|\zeta\|_{0,E}^2 + \frac{1}{4\epsilon_4}\sum_{E\in\tau_h}\|p-p_h\|_{1,E}^2,\end{aligned} \tag{54}$$

$$\begin{aligned}L_2 &= \sum_{e\in\xi_h'}\int_e\sqrt{\frac{\alpha}{2}}|[\![p-p_h]\!]|\sqrt{\frac{2}{\alpha}}|\{\zeta\cdot\mathbf{n}_e\}|\,\mathrm{d}\gamma\\ &\le \epsilon_5\sum_{e\in\xi_h'}\frac{2}{\alpha}\|\{\zeta\cdot\mathbf{n}_e\}\|_{0,e}^2 + \frac{1}{4\epsilon_5}\sum_{e\in\xi_h'}\frac{\alpha}{2}\|[\![p-p_h]\!]\|_{0,e}^2,\end{aligned} \tag{55}$$

$$\begin{aligned}L_3 &= \sum_{e\in\xi_h^{\mathrm{D}}}\int_e\sqrt{\alpha}|p-p_h|\sqrt{\frac{1}{\alpha}}|\zeta\cdot\mathbf{n}_e|\,\mathrm{d}\gamma\\ &\le \epsilon_5\sum_{e\in\xi_h^{\mathrm{D}}}\frac{1}{\alpha}\|\zeta\cdot\mathbf{n}_e\|_{0,e}^2 + \frac{1}{4\epsilon_5}\sum_{e\in\xi_h^{\mathrm{D}}}\alpha\|[\![p-p_h]\!]\|_{0,e}^2.\end{aligned} \tag{56}$$

Since the trace inequality (9) provides $\|q\|_{0,e}^2 \le c\frac{k^2}{h}\|q\|_{0,E}^2$, by using the inequality $(a+b)^2\le 2a^2+2b^2$, we get

$$\sum_{e\in\xi_h'}\frac{2}{\alpha}\|\{\zeta\cdot\mathbf{n}_e\}\|_{0,e}^2 + \sum_{e\in\xi_h^{\mathrm{D}}}\frac{1}{\alpha}\|\zeta\cdot\mathbf{n}_e\|_{0,e}^2 \le c_2\,\frac{k^2}{h}\frac{1}{\alpha}\sum_{E\in\tau_h}\|\zeta\|_{0,E}^2.$$

Consequently,

$$\begin{aligned}|\mathcal{G}(\zeta,\zeta)| &\le A_1+A_2+A_3+L_1+L_2+L_3\\ &\le \left(c_1\epsilon_1+\epsilon_4+\epsilon_5c_2\frac{k^2}{h}\frac{1}{\alpha}\right)\sum_{E\in\tau_h}\|\zeta\|_{0,E}^2\\ &\quad+\epsilon_2\sum_{e\in\xi_h'}\frac{1}{2\alpha}\|[\![\zeta\cdot\mathbf{n}_e]\!]\|_{0,e}^2+\epsilon_3\sum_{e\in\xi_h^{\mathrm{N}}}\frac{1}{\alpha}\|(\zeta\cdot\mathbf{n}_e)\|_{0,e}^2\\ &\quad+\frac{c_1}{4\epsilon_1}\sum_{E\in\tau_h}\|\eta\|_{0,E}^2+\frac{1}{4\epsilon_2}\sum_{e\in\xi_h'}\frac{1}{2\alpha}\|[\![\eta\cdot\mathbf{n}_e]\!]\|_{0,e}^2\\ &\quad+\frac{1}{4\epsilon_3}\sum_{e\in\xi_h^{\mathrm{N}}}\frac{1}{\alpha}\|(\eta\cdot\mathbf{n}_e)\|_{0,e}^2\\ &\quad+\left(\frac{1}{4\epsilon_4}+\frac{1}{4\epsilon_5}+\frac{1}{4\epsilon_5}\right)|\!|\!|\,p-p_h\,|\!|\!|.\end{aligned} \tag{57}$$

Using the elliptic property of K (see Eq. 2), we get

$$\frac{1}{\lambda_M}\sum_{E\in\tau_h}\|\zeta\|_{0,E}^2+\sum_{e\in\xi_h'}\frac{1}{2\alpha}\|[\![\zeta\cdot\mathbf{n}_e]\!]\|_{0,e}^2 + \sum_{e\in\xi_h^{\mathrm{N}}}\frac{1}{\alpha}\|(\zeta\cdot\mathbf{n}_e)\|_{0,e}^2\le|\mathcal{G}(\zeta,\zeta)|. \tag{58}$$

Then Eq. 57 implies

$$\begin{aligned}&\left(\frac{1}{\lambda_M}-c_1\epsilon_1-\epsilon_4-\epsilon_5\,c_2\frac{k^2}{h}\frac{1}{\alpha}\right)\sum_{E\in\tau_h}\|\zeta\|_{0,E}^2\\&+(1-\epsilon_2)\sum_{e\in\xi_h'}\frac{1}{2\alpha}\|[\![\zeta\cdot\mathbf{n}_e]\!]\|_{0,e}^2\\&+(1-\epsilon_3)\sum_{e\in\xi_h^{\mathrm{N}}}\frac{1}{\alpha}\|(\zeta\cdot\mathbf{n}_e)\|_{0,e}^2\\&\le\frac{c_1}{4\epsilon_1}\sum_{E\in\tau_h}\|\eta\|_{0,E}^2+\frac{1}{4\epsilon_2}\sum_{e\in\xi_h'}\frac{1}{2\alpha}\|[\![\eta\cdot\mathbf{n}_e]\!]\|_{0,e}^2\\&+\frac{1}{4\epsilon_3}\sum_{e\in\xi_h^{\mathrm{N}}}\frac{1}{\alpha}\|(\eta\cdot\mathbf{n}_e)\|_{0,e}^2\\&+\left(\frac{1}{4\epsilon_4}+\frac{1}{4\epsilon_5}+\frac{1}{4\epsilon_5}\right)|\!|\!|\,p-p_h\,|\!|\!|^2.\end{aligned} \tag{59}$$

Then, by choosing $\alpha=\frac{\sigma k^2}{h}$ and $\epsilon_i>0, i=1,\ldots,5$ such that $\begin{cases}\left(\frac{1}{\lambda_M}-c_1\epsilon_1-\epsilon_4-\frac{\epsilon_5c_2}{\sigma}\right)>0,\\ \frac{1-\epsilon_2}{\sigma}>0,\\ \frac{1-\epsilon_3}{\sigma}>0,\end{cases}$ which is possible provided that $\begin{cases}c_1\epsilon_1=\epsilon_4=\epsilon_5\frac{c_2}{\sigma}=\frac{1}{6\lambda_M},\\ \epsilon_2=\frac{1}{2},\\ \epsilon_3=\frac{1}{2},\end{cases}$, it turns out that there are constants $C_i>0, i=1,\ldots,6$ independent of k and h such that

$$\begin{aligned}&C_1\sum_{E\in\tau_h}\|\zeta\|_{0,E}^2+C_2\sum_{e\in\xi_h'}\frac{h}{k^2}\|[\![\zeta\cdot\mathbf{n}_e]\!]\|_{0,e}^2\\&+C_3\sum_{e\in\xi_h^{\mathrm{N}}}\frac{h}{k^2}\|(\zeta\cdot\mathbf{n}_e)\|_{0,e}^2\\&\le\underbrace{C_4\sum_{E\in\tau_h}\|\eta\|_{0,E}^2}_{T_1}+\underbrace{C_5\sum_{e\in\xi_h'}\frac{h}{k^2}\|[\![\eta\cdot\mathbf{n}_e]\!]\|_{0,e}^2}_{T_2}\\&+\underbrace{C_5\sum_{e\in\xi_h^{\mathrm{N}}}\frac{h}{k^2}\|(\eta\cdot\mathbf{n}_e)\|_{0,e}^2}_{T_3}+\underbrace{C_6|\!|\!|\,p-p_h\,|\!|\!|^2}_{T_4}.\end{aligned} \tag{60}$$

Consequently, by the approximation result given by Lemma 2, it follows that

$$T_1+T_2+T_3\le C\frac{h^{2\mu-2}}{k^{2s-3}}\sum_{E\in\tau_h}\|\mathbf{u}\|_{s,E}^2.$$

It remains to bound T_4. To this end, we make use of the error estimates given by Eq. 11 to get

$$T_4\le C\frac{h^{2\mu-2}}{k^{2s-3}}\sum_{E\in\tau_h}\|p\|_{s,E}^2.$$

Hence,

$$C_1\sum_{E\in\tau_h}\|\zeta\|_{0,E}^2\le C\frac{h^{2\mu-2}}{k^{2s-3}}\left(\sum_{E\in\tau_h}\|\mathbf{u}\|_{s,E}^2+\sum_{E\in\tau_h}\|p\|_{s,E}^2\right), \tag{61}$$

$$\begin{aligned}&C_2\sum_{e\in\xi_h'}\frac{h}{k^2}\|[\![\zeta\cdot\mathbf{n}_e]\!]\|_{0,e}^2+C_3\sum_{e\in\xi_h^{\mathrm{N}}}\frac{h}{k^2}\|(\zeta\cdot\mathbf{n}_e)\|_{0,e}^2\\&\le C\frac{h^{2\mu-2}}{k^{2s-3}}\left(\sum_{E\in\tau_h}\|\mathbf{u}\|_{s,E}^2+\sum_{E\in\tau_h}\|p\|_{s,E}^2.\right).\end{aligned} \tag{62}$$

This completes the proof. □

Appendix 2: Proof of Proposition 3

Proof of Proposition 3 Let

$$\mathcal{G}(\mathbf{u},\mathbf{v})=\sum_{E\in\tau_h}\int_E K^{-1}\mathbf{u}\cdot\mathbf{v}\,dx+\sum_{e\in\xi_h^{\mathrm{N}}}\frac{1}{\alpha}\int_e(\mathbf{u}\cdot\mathbf{n}_e)(\mathbf{v}\cdot\mathbf{n}_e)\,d\gamma,$$

$$\begin{aligned}\mathcal{F}(p;\mathbf{v})=&-\sum_{E\in\tau_h}\int_E\mathbf{v}\cdot\nabla p\,dx+\sum_{e\in\xi_h'}[\![p]\!]\{\mathbf{v}\cdot\mathbf{n}_e\}\,d\gamma\\&+\sum_{e\in\xi_h^{\mathrm{D}}}p(\mathbf{v}\cdot\mathbf{n}_e)\,d\gamma\\&-\sum_{e\in\xi_h'}\frac{1}{2\alpha}\int_e[\![-(K\nabla p)\cdot\mathbf{n}_e]\!][\![\mathbf{v}\cdot\mathbf{n}_e]\!]\,d\gamma.\end{aligned}$$

Existence and uniqueness of the discrete velocity As the space Σ_h^k has finite dimension, it is sufficient to show the uniqueness of the solution. Let $\mathbf{v}\in\Sigma_h^k$ be such that $\mathcal{G}(\mathbf{v},\mathbf{v})=0$. Then $\sum_{E\in\tau_h}\int_E(K^{-1}\mathbf{v})\cdot\mathbf{v}\,dx=0$. Consequently, from the ellipticity of K, we get $||\mathbf{v}||_{0,E}^2=0\ \forall\ E\in\tau_h$. Hence, $\mathbf{v}\equiv0$.

Error estimates Denote $\eta = \mathbf{u} - \hat{\mathbf{u}}$, $\zeta = \hat{\mathbf{u}} - \mathbf{u}_h$, with $\hat{\mathbf{u}}$ an interpolation of $\mathbf{u}$ satisfying for each component the relation (10) given by Lemma 2. We have

$$\begin{aligned}\mathcal{G}(\zeta,\zeta) &= -\mathcal{G}(\eta,\zeta) + \mathcal{G}(\mathbf{u},\zeta) - \mathcal{G}(\mathbf{u}_h,\zeta)\\ &= -\mathcal{G}(\eta,\zeta) - \mathcal{F}(p-p_h;\zeta).\end{aligned} \tag{63}$$

It follows that

$$|\mathcal{G}(\zeta,\zeta)| \le |\mathcal{G}(\eta,\zeta)| + |\mathcal{F}(p-p_h;\zeta)|. \tag{64}$$

Then

$$\begin{aligned}|\mathcal{G}(\eta,\zeta)| &\le A_1 + A_2,\\ |\mathcal{F}(p-p_h;\zeta)| &\le L_1 + L_2 + L_3 + L_4,\end{aligned} \tag{65}$$

where $A_i, i = 1,\dots 3$, $L_i, i = 1,\dots 4$ are given below and bounded using the algebraic inequality $ab \le \epsilon a^2 + \frac{1}{4\epsilon} b^2$, which is true for any real numbers a and b and $\epsilon > 0$.

$$\begin{aligned}A_1 &= \sum_{E\in\tau_h}\int_E |(K^{-1}\eta)\cdot\zeta|\,\mathrm{d}x\\ &\le c_1 \sum_{E\in\tau_h} \|\eta\|_{0,E}\|\zeta\|_{0,E}\\ &\le c_1\epsilon_1 \sum_{E\in\tau_h}\|\zeta\|^2_{0,E} + \frac{c_1}{4\epsilon_1}\sum_{E\in\tau_h}\|\zeta\|^2_{0,E},\end{aligned}$$

$$\begin{aligned}A_2 &= \sum_{e\in\xi_h^{\mathrm{N}}}\frac{1}{\alpha}\int_e |(\eta\cdot\mathbf{n}_e)(\zeta\cdot\mathbf{n}_e)|\,\mathrm{d}\gamma\\ &\le \epsilon_2 \sum_{e\in\xi_h^{\mathrm{N}}}\frac{1}{\alpha}\|(\zeta\cdot\mathbf{n}_e)\|^2_{0,e} + \frac{1}{4\epsilon_2}\sum_{e\in\xi_h^{\mathrm{N}}}\frac{1}{\alpha}\|(\eta\cdot\mathbf{n}_e)\|^2_{0,e},\end{aligned}$$

$$\begin{aligned}L_1 &= \sum_{E\in\tau_h}\int_E |\zeta\cdot\nabla(p-p_h)|\,\mathrm{d}x\\ &\le \epsilon_3\sum_{E\in\tau_h}\|\zeta\|^2_{0,E} + \frac{1}{4\epsilon_4}\sum_{E\in\tau_h}\|p-p_h\|^2_{1,E},\end{aligned}$$

$$\begin{aligned}L_2 &= \sum_{e\in\xi_h'}\int_e \sqrt{\frac{\alpha}{2}}|[\![p-p_h]\!]|\sqrt{\frac{2}{\alpha}}|\{\zeta\cdot\mathbf{n}_e\}|\,\mathrm{d}\gamma\\ &\le \epsilon_4\sum_{e\in\xi_h'}\frac{2}{\alpha}\|\{\zeta\cdot\mathbf{n}_e\}\|^2_{0,e} + \frac{1}{4\epsilon_4}\sum_{e\in\xi_h'}\frac{\alpha}{2}\|[\![p-p_h]\!]\|^2_{0,e},\end{aligned}$$

$$\begin{aligned}L_3 &= \sum_{e\in\xi_h^{\mathrm{D}}}\int_e \sqrt{\alpha}|p-p_h|\sqrt{\frac{1}{\alpha}}|\zeta\cdot\mathbf{n}_e|\,\mathrm{d}\gamma\\ &\le \epsilon_4\sum_{e\in\xi_h^{\mathrm{D}}}\frac{1}{\alpha}\|\zeta\cdot\mathbf{n}_e\|^2_{0,e} + \frac{1}{4\epsilon_4}\sum_{e\in\xi_h^{\mathrm{D}}}\alpha\|[\![p-p_h]\!]\|^2_{0,e},\end{aligned}$$

$$\begin{aligned}L_4 &= \sum_{e\in\xi_h'}\frac{1}{2\alpha}\int_e |[\![(K\nabla p - p_h)\cdot\mathbf{n}_e]\!][\![\zeta\cdot\mathbf{n}_e]\!]|\,\mathrm{d}\gamma\\ &\le \frac{1}{4\epsilon_5}\sum_{e\in\xi_h'}\frac{1}{2\alpha}\|[\![(K\nabla p - p_h)\cdot\mathbf{n}_e]\!]\|^2_{0,e}\\ &\quad + \epsilon_5\sum_{e\in\xi_h'}\frac{1}{2\alpha}\|[\![\zeta\cdot\mathbf{n}_e]\!]\|^2_{0,e}.\end{aligned}$$

Using inequality $(a+b)^2 \le 2a^2 + 2b^2$ and the trace inequality (9), we obtain

$$\begin{aligned}&\sum_{e\in\xi_h'}\frac{2}{\alpha}\|\{\zeta\cdot\mathbf{n}_e\}\|^2_{0,e} + \sum_{e\in\xi_h^{\mathrm{D}}}\frac{1}{\alpha}\|\zeta\cdot\mathbf{n}_e\|^2_{0,e}\\ &\le c_2\,\frac{k^2}{h}\frac{1}{\alpha}\sum_{E\in\tau_h}\|\zeta\|^2_{0,E}.\end{aligned}$$

Consequently

$$\begin{aligned}|\mathcal{G}(\zeta,\zeta)| &\le A_1 + A_2 + L_1 + L_2 + L_3 + L_4\\ &\le \left(c_1\epsilon_1 + \epsilon_3 + \epsilon_4\,c_2\,\frac{k^2}{h}\frac{1}{\alpha}\right)\sum_{E\in\tau_h}\|\zeta\|^2_{0,E}\\ &\quad + \epsilon_2\sum_{e\in\xi_h^{\mathrm{N}}}\frac{1}{\alpha}\|(\zeta\cdot\mathbf{n}_e)\|^2_{0,e}\\ &\quad + \epsilon_5\sum_{e\in\xi_h'}\frac{1}{2\alpha}\|[\![\zeta\cdot\mathbf{n}_e]\!]\|^2_{0,e}\\ &\quad + \frac{c_1}{4\epsilon_1}\sum_{E\in\tau_h}\|\eta\|^2_{0,E} + \frac{1}{4\epsilon_2}\sum_{e\in\xi_h^{\mathrm{N}}}\frac{1}{\alpha}\|(\eta\cdot\mathbf{n}_e)\|^2_{0,e}\\ &\quad + \left(\frac{1}{4\epsilon_3} + \frac{1}{4\epsilon_4} + \frac{1}{4\epsilon_5}\right)|\!|\!|\,p-p_h\,|\!|\!|.\end{aligned} \tag{66}$$

Using the ellipticity of K, we get

$$\frac{1}{\lambda_M}\sum_{E\in\tau_h}\|\zeta\|^2_{0,E} + \sum_{e\in\xi_h^{\mathrm{N}}}\frac{1}{\alpha}\|(\zeta\cdot\mathbf{n}_e)\|^2_{0,e} \le |\mathcal{G}(\zeta,\zeta)|. \tag{67}$$

By Eq. 66, this gives

$$\left(\frac{1}{\lambda_M} - c_1\epsilon_1 - \epsilon_3 - \epsilon_4\, c_2\, \frac{k^2}{h}\frac{1}{\alpha}\right) \sum_{E\in\tau_h} \|\zeta\|^2_{0,E}$$

$$+ (1-\epsilon_2) \sum_{e\in\xi_h^{\mathrm{N}}} \frac{1}{\alpha}\|(\zeta\cdot\mathbf{n}_e)\|^2_{0,e} + \epsilon_5 \sum_{e\in\xi_h'} \frac{1}{2\alpha}\|[\![\zeta\cdot\mathbf{n}_e]\!]\|^2_{0,e}$$

$$\le \frac{c_1}{4\epsilon_1}\sum_{E\in\tau_h}\|\eta\|^2_{0,E} + \frac{1}{4\epsilon_2}\sum_{e\in\xi_h^{\mathrm{N}}}\frac{1}{\alpha}\|(\eta\cdot\mathbf{n}_e)\|^2_{0,e}$$

$$+ \left(\frac{1}{4\epsilon_4}+\frac{1}{4\epsilon_5}+\frac{1}{4\epsilon_5}\right)|\!|\!| p-p_h |\!|\!|^2$$

$$+ \epsilon_5 \sum_{e\in\xi_h'} \frac{1}{\alpha}\|[\![\zeta\cdot\mathbf{n}_e]\!]\|^2_{0,e}. \tag{68}$$

Using the inequality $\sum_{e\in\xi_h'}\|[\![\zeta\cdot\mathbf{n}_e]\!]\|^2_{0,e} \le c_2\frac{k^2}{h}\sum_{E\in\tau_h}\|\eta\|^2_{0,E}$, we get

$$\left(\frac{1}{\lambda_M} - c_1\epsilon_1 - \epsilon_3 - (\epsilon_4+\epsilon_5)\, c_2\, \frac{k^2}{h}\frac{1}{\alpha}\right) \sum_{E\in\tau_h} \|\zeta\|^2_{0,E}$$

$$+ (1-\epsilon_2) \sum_{e\in\xi_h^{\mathrm{N}}} \frac{1}{\alpha}\|(\zeta\cdot\mathbf{n}_e)\|^2_{0,e} + \epsilon_5 \sum_{e\in\xi_h'} \frac{1}{2\alpha}\|[\![\zeta\cdot\mathbf{n}_e]\!]\|^2_{0,e}$$

$$\le \frac{c_1}{4\epsilon_1}\sum_{E\in\tau_h}\|\eta\|^2_{0,E} + \frac{1}{4\epsilon_2}\sum_{e\in\xi_h^{\mathrm{N}}}\frac{1}{\alpha}\|(\eta\cdot\mathbf{n}_e)\|^2_{0,e}$$

$$+ \left(\frac{1}{4\epsilon_4}+\frac{1}{4\epsilon_5}+\frac{1}{4\epsilon_5}\right)|\!|\!| p-p_h |\!|\!|^2. \tag{69}$$

Choosing $\alpha = \frac{\sigma k^2}{h}$ and $\epsilon_i > 0, i = 1,\ldots,5$ such that

$$\begin{cases} \left(\dfrac{1}{\lambda_M} - c_1\epsilon_1 - \epsilon_3 - (\epsilon_4+\epsilon_5)\dfrac{c_2}{\sigma}\right) > 0, \\ \qquad\qquad\qquad\qquad \dfrac{1-\epsilon_2}{\sigma} > 0, \end{cases}$$

which is possible provided that

$$\begin{cases} c_1\epsilon_1 = \epsilon_3 = \epsilon_4\dfrac{c_2}{\sigma} = \epsilon_5\dfrac{c_2}{\sigma} = \dfrac{1}{8\lambda_M} \\ \epsilon_2 = \dfrac{1}{2}. \end{cases},$$

it turns out that one can find some constants $C_i > 0$, $i = 1,\ldots,6$ independent of k and h such that

$$C_1\sum_{E\in\tau_h}\|\zeta\|^2_{0,E} + C_2\sum_{e\in\xi_h'}\frac{h}{k^2}\|[\![\zeta\cdot\mathbf{n}_e]\!]\|^2_{0,e}$$

$$+ C_3\sum_{e\in\xi_h^{\mathrm{N}}}\frac{h}{k^2}\|(\zeta\cdot\mathbf{n}_e)\|^2_{0,e}$$

$$\le \underbrace{C_4\sum_{E\in\tau_h}\|\eta\|^2_{0,E}}_{T_2} + \underbrace{C_5\sum_{e\in\xi_h^{\mathrm{N}}}\frac{h}{k^2}\|(\eta\cdot\mathbf{n}_e)\|^2_{0,e}}_{T_1}$$

$$+ \underbrace{C_6|\!|\!| p-p_h |\!|\!|^2}_{T_3}. \tag{70}$$

By the approximation result of Lemma 2, it follows that

$$T_1 + T_2 \le C\frac{h^{2\mu-2}}{k^{2s-3}}\sum_{E\in\tau_h}\|\mathbf{u}\|^2_{s,E}.$$

The last term (i.e., T_3) is treated using the error estimate (11). □

Appendix 3: Proof of Proposition 5

Proof of Proposition 5 Summing Eq. 37 over all elements $E \in \tau_h$, we get

$$\sum_{E\in\tau_h}\int_E K^{-1}\mathbf{u}_h\cdot\mathbf{v}_h\,\mathrm{d}x + \sum_{E\in\tau_h}\frac{1}{2\alpha}\int_{\partial E\cap\partial E'}\mathbf{u}_h\cdot\mathbf{n}\,\mathbf{v}_h\cdot\mathbf{n}\,\mathrm{d}\gamma$$

$$+ \sum_{e\in\xi_h^{\mathrm{N}}}\frac{1}{\alpha}\int_e \mathbf{u}_h\cdot\mathbf{n}_e\,\mathbf{v}_h\cdot\mathbf{n}_e\,\mathrm{d}\gamma$$

$$= \sum_{E\in\tau_h}\int_E(-\nabla p_h)\cdot\mathbf{v}_h\,\mathrm{d}x + \sum_{e\in\xi_h'}\int_e [\![p_h]\!]\{\mathbf{v}_h\cdot\mathbf{n}_e\}\,\mathrm{d}\gamma$$

$$- \sum_{E\in\tau_h}\frac{1}{2\alpha}\int_{\partial E\cap\partial E'}(K'\nabla p_h')\cdot\mathbf{n}\,\mathbf{v}_h\cdot\mathbf{n}\,\mathrm{d}\gamma$$

$$+ \sum_{e\in\xi_h^{\mathrm{D}}}\int_e (p_h - p_{\mathrm{D}})\,\mathbf{v}_h\cdot\mathbf{n}_e\,\mathrm{d}\gamma$$

$$- \sum_{e\in\xi_h^{\mathrm{N}}}\frac{1}{\alpha}\int_e g_{\mathrm{N}}\,\mathbf{v}_h\cdot\mathbf{n}_e\,\mathrm{d}\gamma. \tag{71}$$

Using the identity $ab + cd = \frac{1}{2}(a+c)(c+d) + \frac{1}{2}(a-c)(b-d)$ we have

$$\sum_{E\in\tau_h} \frac{1}{2\alpha} \int_{\partial E\cap\partial E'} \mathbf{u}_h\cdot\mathbf{n}\,\mathbf{v}_h\cdot\mathbf{n}\,\mathrm{d}\gamma$$
$$= \sum_{e\in\xi_h'} \frac{1}{4\alpha} \int_e [\![\mathbf{u}_h\cdot\mathbf{n}_e]\!][\![\mathbf{v}_h\cdot\mathbf{n}_e]\!]\,\mathrm{d}\gamma$$
$$+ \sum_{e\in\xi_h'} \frac{1}{\alpha} \int_e \{\mathbf{u}_h\cdot\mathbf{n}_e\}\{\mathbf{v}_h\cdot\mathbf{n}_e\}\,\mathrm{d}\gamma \tag{72}$$

and

$$\sum_{E\in\tau_h} \frac{1}{2\alpha} \int_{\partial E\cap\partial E'} (K'\nabla p_h')\cdot\mathbf{n}\,\mathbf{v}_h\cdot\mathbf{n}\,\mathrm{d}\gamma$$
$$= \sum_{e\in\xi_h'} \frac{1}{4\alpha} \int_e [\![K\nabla p_h\cdot\mathbf{n}_e]\!][\![\mathbf{v}_h\cdot\mathbf{n}_e]\!]\,\mathrm{d}\gamma$$
$$- \sum_{e\in\xi_h'} \frac{1}{\alpha} \int_e \{K\nabla p_h\cdot\mathbf{n}_e\}\{\mathbf{v}_h\cdot\mathbf{n}_e\}\,\mathrm{d}\gamma.$$

Hence, problem (37) can be rewritten as

$$\mathcal{G}(\mathbf{u}_h,\mathbf{v}_h) = l(\mathbf{v}_h) \quad \forall \mathbf{v}_h\in\Sigma_h^k, \tag{73}$$

where

$$\mathcal{G}(\mathbf{u},\mathbf{v}) = \sum_{E\in\tau_h}\int_E K^{-1}\mathbf{u}\cdot\mathbf{v}\,\mathrm{d}x$$
$$+ \sum_{e\in\xi_h'} \frac{1}{4\alpha}\int_e [\![\mathbf{u}\cdot\mathbf{n}_e]\!][\![\mathbf{v}\cdot\mathbf{n}_e]\!]\,\mathrm{d}\gamma$$
$$+ \sum_{e\in\xi_h'} \frac{1}{\alpha}\int_e \{\mathbf{u}\cdot\mathbf{n}_e\}\{\mathbf{v}\cdot\mathbf{n}_e\}\,\mathrm{d}\gamma$$
$$+ \sum_{e\in\xi_h^{\mathrm{N}}} \frac{1}{\alpha}\int_e \mathbf{u}\cdot\mathbf{n}_e\,\mathbf{v}\cdot\mathbf{n}_e\,\mathrm{d}\gamma, \tag{74}$$

$$l(\mathbf{v}) = \sum_{E\in\tau_h}\int_E (-\nabla p)\cdot\mathbf{v}\,\mathrm{d}x$$
$$- \sum_{e\in\xi_h'} \frac{1}{4\alpha}\int_e [\![K\nabla p\cdot\mathbf{n}_e]\!][\![\mathbf{v}\cdot\mathbf{n}_e]\!]\,\mathrm{d}\gamma$$
$$+ \sum_{e\in\xi_h'} \frac{1}{\alpha}\int_e \{K\nabla p\cdot\mathbf{n}_e\}\{\mathbf{v}\cdot\mathbf{n}_e\}\,\mathrm{d}\gamma$$
$$+ \sum_{e\in\xi_h'} \int_e [\![p]\!]\{\mathbf{v}\cdot\mathbf{n}_e\}\,\mathrm{d}\gamma$$
$$+ \sum_{e\in\xi_h^{\mathrm{D}}} \int_e (p_h - p_{\mathrm{D}})\,\mathbf{v}\cdot\mathbf{n}_e\,\mathrm{d}\gamma$$
$$- \sum_{e\in\xi_h^{\mathrm{N}}} \frac{1}{\alpha}\int_e g_{\mathrm{N}}\,\mathbf{v}\cdot\mathbf{n}_e\,\mathrm{d}\gamma. \tag{75}$$

Proceeding as in the two previous propositions, we can show that this problem has a unique solution. Let us now estimate the errors. For a given function p, introduce the following linear form:

$$\mathcal{F}(p;\mathbf{v}) = \sum_{E\in\tau_h}\int_E (-\nabla p)\cdot\mathbf{v}\,\mathrm{d}x$$
$$- \sum_{e\in\xi_h'} \frac{1}{4\alpha}\int_e [\![K\nabla p\cdot\mathbf{n}_e]\!][\![\mathbf{v}\cdot\mathbf{n}_e]\!]\,\mathrm{d}\gamma$$
$$+ \sum_{e\in\xi_h'} \int_e [\![p]\!]\{\mathbf{v}\cdot\mathbf{n}_e\}\,\mathrm{d}\gamma$$
$$+ \sum_{e\in\xi_h'} \frac{1}{\alpha}\int_e \{K\nabla p\cdot\mathbf{n}_e\}\{\mathbf{v}\cdot\mathbf{n}_e\}\,\mathrm{d}\gamma$$
$$+ \sum_{e\in\xi_h^{\mathrm{D}}} \int_e p\,\mathbf{v}\cdot\mathbf{n}_e\,\mathrm{d}\gamma. \tag{76}$$

Denote $\eta = \mathbf{u} - \hat{\mathbf{u}}, \quad \zeta = \hat{\mathbf{u}} - \mathbf{u}_h$, with $\hat{\mathbf{u}}$ an interpolate of $\mathbf{u}$ satisfying for each component the relation (10) given by Lemma 2. Since,

$$\mathcal{G}(\zeta,\zeta) = -\mathcal{G}(\eta,\zeta) + \mathcal{G}(\mathbf{u},\zeta) - \mathcal{G}(\mathbf{u}_h,\zeta)$$
$$= -\mathcal{G}(\eta,\zeta) - \mathcal{F}(p-p_h;\zeta), \tag{77}$$

it follows that

$$|\mathcal{G}(\zeta,\zeta)| \le |\mathcal{G}(\eta,\zeta)| + |\mathcal{F}(p-p_h;\zeta)|. \tag{78}$$

Consequently,

$$|\mathcal{G}(\eta,\zeta)| \le A_1 + A_2 + A_3 + A_4,$$
$$|\mathcal{F}(p-p_h;\zeta)| \le L_1 + L_2 + L_3 + L_4 + L_5, \tag{79}$$

where $A_i, i = 1,\ldots 4$ and $L_i, i = 1,\ldots 5$ are given below and are bounded using the algebraic inequality $ab \le \epsilon a^2 + \frac{1}{4\epsilon}b^2$, which is valid for any real numbers a and b and $\epsilon > 0$.

$$A_1 = \sum_{E\in\tau_h}\int_E |(K^{-1}\eta)\cdot\zeta|\,\mathrm{d}x$$
$$\le c_1 \sum_{E\in\tau_h} \|\eta\|_{0,E}\|\zeta\|_{0,E}$$
$$\le c_1\epsilon_1 \sum_{E\in\tau_h}\|\zeta\|_{0,E}^2 + \frac{c_1}{4\epsilon_1}\sum_{E\in\tau_h}\|\eta\|_{0,E}^2,$$

$$A_2 = \sum_{e\in\xi_h'} \frac{1}{4\alpha}\int_e |[\![\eta\cdot\mathbf{n}_e]\!][\![\zeta\cdot\mathbf{n}_e]\!]|\,\mathrm{d}\gamma$$

$$\le \epsilon_2 \sum_{e\in\xi_h'} \frac{1}{2\alpha}\|[\![\zeta\cdot\mathbf{n}_e]\!]\|_{0,e}^2 + \frac{1}{4\epsilon_2}\sum_{e\in\xi_h'}\frac{1}{2\alpha}\|[\![\eta\cdot\mathbf{n}_e]\!]\|_{0,e}^2,$$

$$A_3 = \sum_{e\in\xi_h'} \frac{1}{\alpha}\int_e |\{\eta\cdot\mathbf{n}_e\}\{\zeta\cdot\mathbf{n}_e\}|\,\mathrm{d}\gamma$$

$$\le \epsilon_3 \sum_{e\in\xi_h'} \frac{1}{\alpha}\|\{\zeta\cdot\mathbf{n}_e\}\|_{0,e}^2 + \frac{1}{4\epsilon_3}\sum_{e\in\xi_h'}\frac{1}{\alpha}\|\{\eta\cdot\mathbf{n}_e\}\|_{0,e}^2,$$

$$A_4 = \sum_{e\in\xi_h^{\mathrm{N}}} \frac{1}{\alpha}\int_e |(\eta\cdot\mathbf{n}_e)(\zeta\cdot\mathbf{n}_e)|\,\mathrm{d}\gamma$$

$$\le \epsilon_4 \sum_{e\in\xi_h^{\mathrm{N}}} \frac{1}{\alpha}\|(\zeta\cdot\mathbf{n}_e)\|_{0,e}^2 + \frac{1}{4\epsilon_4}\sum_{e\in\xi_h^{\mathrm{N}}}\frac{1}{\alpha}\|(\eta\cdot\mathbf{n}_e)\|_{0,e}^2,$$

$$L_1 = \sum_{E\in\tau_h}\int_E |\zeta\cdot\nabla(p-p_h)|\,\mathrm{d}x$$

$$\le \epsilon_5 \sum_{E\in\tau_h}\|\zeta\|_{0,E}^2 + \frac{1}{4\epsilon_5}\sum_{E\in\tau_h}\|p-p_h\|_{1,E}^2,$$

$$L_2 = \sum_{e\in\xi_h'}\int_e \sqrt{\frac{\alpha}{2}}|[\![p-p_h]\!]|\sqrt{\frac{2}{\alpha}}|\{\zeta\cdot\mathbf{n}_e\}|\,\mathrm{d}\gamma$$

$$\le \epsilon_6 \sum_{e\in\xi_h'}\frac{2}{\alpha}\|\{\zeta\cdot\mathbf{n}_e\}\|_{0,e}^2 + \frac{1}{4\epsilon_6}\sum_{e\in\xi_h'}\frac{\alpha}{2}\|[\![p-p_h]\!]\|_{0,e}^2,$$

$$L_3 = \sum_{e\in\xi_h^{\mathrm{D}}}\int_e \sqrt{\alpha}|p-p_h|\sqrt{\frac{1}{\alpha}}|\zeta\cdot\mathbf{n}_e|\,\mathrm{d}\gamma$$

$$\le \epsilon_7 \sum_{e\in\xi_h^{\mathrm{D}}}\frac{1}{\alpha}\|\zeta\cdot\mathbf{n}_e\|_{0,e}^2 + \frac{1}{4\epsilon_7}\sum_{e\in\xi_h^{\mathrm{D}}}\alpha\|[\![p-p_h]\!]\|_{0,e}^2,$$

$$L_4 = \sum_{e\in\xi_h'}\frac{1}{4\alpha}\int_e |[\![(K\nabla p-p_h)\cdot\mathbf{n}_e]\!][\![\zeta\cdot\mathbf{n}_e]\!]|\,\mathrm{d}\gamma$$

$$\le \frac{1}{4\epsilon_8}\sum_{e\in\xi_h'}\frac{1}{4\alpha}\|[\![(K\nabla p-p_h)\cdot\mathbf{n}_e]\!]\|_{0,e}^2$$

$$+\epsilon_8\sum_{e\in\xi_h'}\frac{1}{4\alpha}\|[\![\zeta\cdot\mathbf{n}_e]\!]\|_{0,e}^2.$$

$$L_5 = \sum_{e\in\xi_h'}\frac{1}{2\alpha}\int_e |\{(K\nabla p-p_h)\cdot\mathbf{n}_e\}\{\zeta\cdot\mathbf{n}_e\}|\,\mathrm{d}\gamma$$

$$\le \frac{1}{4\epsilon_9}\sum_{e\in\xi_h'}\frac{1}{2\alpha}\|\{(K\nabla p-p_h)\cdot\mathbf{n}_e\}\|_{0,e}^2$$

$$+\epsilon_9\sum_{e\in\xi_h'}\frac{1}{2\alpha}\|\{\zeta\cdot\mathbf{n}_e\}\|_{0,e}^2.$$

Observing that there exists a constant $c_2 > 0$ independent of h and k such that

$$\sum_{e\in\xi_h^{\mathrm{D}}}\frac{1}{\alpha}\|\zeta\cdot\mathbf{n}_e\|_{0,e}^2 \le c_2\,\frac{k^2}{h}\frac{1}{\alpha}\sum_{E\in\tau_h}\|\zeta\|_{0,E}^2,$$

we get

$$\begin{aligned}
|\mathcal{G}(\zeta,\zeta)| &\le A_1+A_2+A_3+A_4+L_1+L_2+L_3+L_4+L_5\\
&\le \left(c_1\epsilon_1+\epsilon_5+\epsilon_7\,c_2\,\frac{k^2}{h}\frac{1}{\alpha}\right)\sum_{E\in\tau_h}\|\zeta\|_{0,E}^2\\
&\quad+\left(\frac{\epsilon_2}{2}+\frac{\epsilon_8}{4}\right)\sum_{e\in\xi_h'}\frac{1}{\alpha}\|[\![\zeta\cdot\mathbf{n}_e]\!]\|_{0,e}^2\\
&\quad+\left(\epsilon_3+2\epsilon_6+\frac{\epsilon_9}{2}\right)\sum_{e\in\xi_h'}\frac{1}{\alpha}\|\{\zeta\cdot\mathbf{n}_e\}\|_{0,e}^2\\
&\quad+\epsilon_4\sum_{e\in\xi_h^{\mathrm{N}}}\frac{1}{\alpha}\|(\zeta\cdot\mathbf{n}_e)\|_{0,e}^2+\frac{c_1}{4\epsilon_1}\sum_{E\in\tau_h}\|\eta\|_{0,E}^2\\
&\quad+\frac{1}{4\epsilon_2}\sum_{e\in\xi_h'}\frac{1}{2\alpha}\|[\![\eta\cdot\mathbf{n}_e]\!]\|_{0,e}^2\\
&\quad+\frac{1}{4\epsilon_3}\sum_{e\in\xi_h'}\frac{1}{\alpha}\|\{\eta\cdot\mathbf{n}_e\}\|_{0,e}^2\\
&\quad+\frac{1}{4\epsilon_4}\sum_{e\in\xi_h^{\mathrm{N}}}\frac{1}{\alpha}\|(\eta\cdot\mathbf{n}_e)\|_{0,e}^2\\
&\quad+\left(\frac{1}{4\epsilon_5}+\frac{1}{4\epsilon_6}+\frac{1}{4\epsilon_7}+\frac{1}{8\epsilon_9}+\frac{1}{16\epsilon_8}\right)\\
&\quad\times|\!|\!|\,p-p_h\,|\!|\!|. \qquad (80)
\end{aligned}$$

The ellipticity property of K yields

$$\begin{aligned}
&\frac{1}{\lambda_M}\sum_{E\in\tau_h}\|\zeta\|_{0,E}^2+\sum_{e\in\xi_h'}\frac{1}{4\alpha}\|[\![\zeta\cdot\mathbf{n}_e]\!]\|_{0,e}^2+\frac{1}{\alpha}\|\{\zeta\cdot\mathbf{n}_e\}\|_{0,e}^2\\
&+\sum_{e\in\xi_h^{\mathrm{N}}}\frac{1}{\alpha}\|(\eta\cdot\mathbf{n}_e)\|_{0,e}^2 \le \mathcal{G}(\zeta,\zeta). \qquad (81)
\end{aligned}$$

Combining Eqs. 80 and 81, we get

$$\left(\frac{1}{\lambda_M}-c_1\epsilon_1-\epsilon_5-\epsilon_7\,c_2\,\frac{k^2}{h}\frac{1}{\alpha}\right)\sum_{E\in\tau_h}\|\zeta\|_{0,E}^2$$

$$+\left(\frac{1}{4}-\frac{\epsilon_2}{2}-\frac{\epsilon_8}{4}\right)\sum_{e\in\xi_h'}\frac{1}{\alpha}\|[\![\zeta\cdot\mathbf{n}_e]\!]\|_{0,e}^2$$

$$+\left(1-\epsilon_3-2\epsilon_6-\frac{\epsilon_9}{2}\right)\sum_{e\in\xi_h'}\frac{1}{\alpha}\|\{\zeta\cdot\mathbf{n}_e\}\|_{0,e}^2$$

$$+(1-\epsilon_4)\sum_{e\in\xi_h^{\mathrm{N}}}\frac{1}{\alpha}\|(\zeta\cdot\mathbf{n}_e)\|_{0,e}^2$$

$$\leq\frac{c_1}{4\epsilon_1}\sum_{E\in\tau_h}\|\eta\|_{0,E}^2+\frac{1}{4\epsilon_2}\sum_{e\in\xi_h'}\frac{1}{2\alpha}\|[\![\eta\cdot\mathbf{n}_e]\!]\|_{0,e}^2$$

$$+\frac{1}{4\epsilon_3}\sum_{e\in\xi_h'}\frac{1}{\alpha}\|\{\eta\cdot\mathbf{n}_e\}\|_{0,e}^2+\frac{1}{4\epsilon_4}\sum_{e\in\xi_h^{\mathrm{N}}}\frac{1}{\alpha}\|(\eta\cdot\mathbf{n}_e)\|_{0,e}^2$$

$$+\left(\frac{1}{4\epsilon_5}+\frac{1}{4\epsilon_6}+\frac{1}{4\epsilon_7}+\frac{1}{8\epsilon_8}+\frac{1}{16\epsilon_9}\right)$$

$$\times|\!|\!|\,p-p_h\,|\!|\!|. \tag{82}$$

Choosing $\alpha=\frac{\sigma k^2}{h}$ and $\epsilon_i>0, i=1,\ldots,9$ such that $\begin{cases}\left(\frac{1}{\lambda_M}-c_1\epsilon_1-\epsilon_5-\epsilon_7\,c_2\,\frac{k^2}{h}\frac{1}{\alpha}\right)>0,\\ \left(\frac{1}{4}-\frac{\epsilon_2}{2}-\frac{\epsilon_8}{4}\right)>0,\\ \left(1-\epsilon_3-2\epsilon_6-\frac{\epsilon_9}{2}\right)>0,\\ (1-\epsilon_4)>0,\end{cases}$ which is possible, provided that $\begin{cases}c_1\epsilon_1=\epsilon_5=\epsilon_7\frac{c_2}{\sigma}=\frac{1}{6\lambda_M},\\ \frac{\epsilon_2}{2}=\frac{\epsilon_8}{4}=\frac{1}{8},\\ \epsilon_3=2\epsilon_6=\frac{\epsilon_9}{2}=\frac{1}{6},\\ \epsilon_4=\frac{1}{2},\end{cases}$ it turns out that one can find constants $C_i>0, i=1,\ldots,9$ independents of k and h such that

$$C_1\sum_{E\in\tau_h}\|\zeta\|_{0,E}^2+C_2\sum_{e\in\xi_h'}\frac{h}{k^2}\|[\![\zeta\cdot\mathbf{n}_e]\!]\|_{0,e}^2$$

$$+C_3\sum_{e\in\xi_h'}\frac{h}{k^2}\|\{\zeta\cdot\mathbf{n}_e\}\|_{0,e}^2$$

$$+C_4\sum_{e\in\xi_h^{\mathrm{N}}}\frac{h}{k^2}\|(\zeta\cdot\mathbf{n}_e)\|_{0,e}^2$$

$$\leq\underbrace{C_9|\!|\!|\,p-p_h\,|\!|\!|^2}_{T_2}$$

$$+\underbrace{\begin{pmatrix}C_5\sum_{E\in\tau_h}\|\eta\|_{0,E}^2+C_6\sum_{e\in\xi_h'}\frac{h}{k^2}\|[\![\eta\cdot\mathbf{n}_e]\!]\|_{0,e}^2\\ +C_7\sum_{e\in\xi_h'}\frac{h}{k^2}\|\{\eta\cdot\mathbf{n}_e\}\|_{0,e}^2\\ +C_8\sum_{e\in\xi_h^{\mathrm{N}}}\frac{h}{k^2}\|(\eta\cdot\mathbf{n}_e)\|_{0,e}^2\end{pmatrix}}_{T_1}. \tag{83}$$

We only need to give upper bound to T_1 and T_2 to conclude.

Using the approximation result given by Lemma 2, we get

$$T_1\leq C\frac{h^{2\mu-2}}{k^{2s-3}}\sum_{E\in\tau_h}\|\mathbf{u}\|_{s,E}^2.$$

The bound of the last term, T_2, is directly given by the convergence result (Eq. 11). □

Appendix 4: Preliminaries tools for estimation of α

In order to estimate the α in the proposed velocity reconstructions, we need the following estimates:

Lemma 3 *Define for any $E\in\tau_h$, the quantity*

$$\kappa_E=\frac{(k+1)(k+d)}{4\lambda_m^E d}\frac{|\partial E|}{|E|}, \tag{84}$$

where d and λ_m^E are defined in Section 2.1.

Then for any positive real numbers $\epsilon_1,\epsilon_2,\epsilon_3,\epsilon_4,\epsilon_5$, the following inequality hold:

$$\left|\sum_{E\in\tau_h}\int_E-\nabla p_h\cdot\mathbf{u}_h\,\mathrm{d}x\right|\leq\sum_{E\in\tau_h}\epsilon_1\int_E K^{-1}\mathbf{u}_h\cdot\mathbf{u}_h\,\mathrm{d}x$$

$$+\sum_{E\in\tau_h}\frac{1}{4\epsilon_1}\int_E K\nabla p_h\cdot\nabla p_h\,\mathrm{d}x, \tag{85}$$

$$\left|\sum_{e\in\xi_h'}\int_e[\![p_h]\!]\{\mathbf{u}\cdot\mathbf{n}_e\}\,\mathrm{d}\gamma+\sum_{e\in\xi_h^{\mathrm{D}}}\int_e(p_h-p_{\mathrm{D}})\mathbf{u}\cdot\mathbf{n}_e\,\mathrm{d}\gamma\right|$$

$$\leq\sum_{e\in\xi_h'}\epsilon_2\int_e[\![p_h]\!]^2\,\mathrm{d}\gamma+\sum_{e\in\xi_h^{\mathrm{D}}}\epsilon_2\int_e(p_h-p_{\mathrm{D}})^2\,\mathrm{d}\gamma$$

$$+\sum_{E\in\tau_h}\frac{\kappa_E}{\epsilon_2}\int_E K^{-1}\mathbf{u}_h\cdot\mathbf{u}_h\,\mathrm{d}x, \tag{86}$$

$$\left|-\sum_{e\in\xi_h^{\mathrm{N}}}\frac{1}{\alpha}\int_e g_{\mathrm{N}}\mathbf{u}_h\cdot\mathbf{n}_e\,\mathrm{d}\gamma\right|\leq\sum_{e\in\xi_h^{\mathrm{N}}}\frac{1}{4\epsilon_3\alpha}\int_e(g_{\mathrm{N}})^2\,\mathrm{d}\gamma$$

$$+\sum_{e\in\xi_h^{\mathrm{N}}}\frac{\epsilon_3}{\alpha}\int_e(\mathbf{u}_h\cdot\mathbf{n}_e)^2\,\mathrm{d}\gamma, \tag{87}$$

$$\left|-\sum_{e\in\xi_h'}\frac{1}{2\alpha}\int_e[\![-K\nabla p_h\cdot\mathbf{n}_e]\!][\![\mathbf{u}_h\cdot\mathbf{n}_e]\!]\,\mathrm{d}\gamma\right|$$
$$\leq\sum_{e\in\xi_h'}\frac{\epsilon_4}{2\alpha}\int_e[\![-K\nabla p_h\cdot\mathbf{n}_e]\!]^2\,\mathrm{d}\gamma$$
$$+\sum_{e\in\xi_h'}\frac{1}{2\alpha 4\epsilon_4}\int_e[\![\mathbf{u}_h\cdot\mathbf{n}_e]\!]^2\,\mathrm{d}\gamma,\tag{88}$$

$$\left|\sum_{e\in\xi_h'}\frac{1}{\alpha}\int_e\{K\nabla p_h\cdot\mathbf{n}_e\}\{\mathbf{u}_h\cdot\mathbf{n}_e\}\,\mathrm{d}\gamma\right|$$
$$\leq\sum_{e\in\xi_h'}\frac{\epsilon_5}{\alpha}\int_e\{K\nabla p_h\cdot\mathbf{n}_e\}^2\,\mathrm{d}\gamma$$
$$+\sum_{e\in\xi_h'}\frac{1}{\alpha 4\epsilon_5}\int_e\{\mathbf{u}_h\cdot\mathbf{n}_e\}^2\,\mathrm{d}\gamma,\tag{89}$$

$$\left|-\sum_{e\in\xi_h'}\frac{1}{2\alpha}\int_e[\![-K\nabla p_h\cdot\mathbf{n}_e]\!][\![\mathbf{u}_h\cdot\mathbf{n}_e]\!]\,\mathrm{d}\gamma\right|$$
$$\leq\sum_{e\in\xi_h'}\frac{\epsilon_4}{2\alpha}\int_e[\![-K\nabla p_h\cdot\mathbf{n}_e]\!]^2\,\mathrm{d}\gamma$$
$$+\sum_{E\in\tau_h}\frac{\kappa_E}{\alpha\epsilon_4}\int_E K^{-1}\mathbf{u}_h\cdot\mathbf{u}_h\,\mathrm{d}x.\tag{90}$$

Proof Simple application of the algebraic inequality $ab\leq\epsilon a^2+\frac{1}{4\epsilon}b^2$ (valid for any $\epsilon>0$) and the inverse inequality (see Lemma 1). □

Appendix 5: Proof of Proposition 2

Proof Taking $\mathbf{v}_h=\mathbf{u}_h$ in Eq. 27 and treating the right-hand side using Eqs. 85–87 of Lemma 3, we get:

$$\sum_{E\in\tau_h}(1-\epsilon_1-\frac{\kappa_E}{\epsilon_2})\int_E K^{-1}\mathbf{u}_h\cdot\mathbf{u}_h\,\mathrm{d}x$$
$$+\sum_{e\in\xi_h'}\frac{1}{2\alpha}\int_e[\![\mathbf{u}_h\cdot\mathbf{n}_e]\!]^2\,\mathrm{d}\gamma+\sum_{e\in\xi_h^{\mathrm{N}}}\frac{1-\epsilon_3}{\alpha}\int_e(\mathbf{u}_h\cdot\mathbf{n}_e)^2\,\mathrm{d}\gamma$$
$$\leq\sum_{E\in\tau_h}\frac{1}{4\epsilon_1}\int_E K\nabla p_h\cdot\nabla p_h\,\mathrm{d}x+\sum_{e\in\xi_h'}\epsilon_2\int_e[\![p_h]\!]^2\,\mathrm{d}\gamma$$
$$+\sum_{e\in\xi_h^{\mathrm{D}}}\epsilon_2\int_e(p_h-p_{\mathrm{D}})^2\,\mathrm{d}\gamma+\sum_{e\in\xi_h^{\mathrm{N}}}\frac{1}{4\epsilon_3\alpha}\int_e(g_{\mathrm{N}})^2\,\mathrm{d}\gamma\tag{91}$$

Hence, the required stability holds provided there exists a constant c such that

$$\begin{cases}1-\epsilon_1-\dfrac{\kappa_E}{\epsilon_2}>0,\\ 1-\epsilon_3>0,\\ \dfrac{1}{4\epsilon_1}\leq 1,\\ 2\epsilon_2=c\times\beta,\end{cases}$$

where β is the one used when solving pressure equation.

Since for $c\geq\frac{4\kappa_E}{3\beta}$ we can always find $\epsilon_i, i=1,2,3$ satisfying the above assumptions, it follows that α is independent of β. □

Appendix 6: Proof of Proposition 4

Proof Taking $\mathbf{v}_h=\mathbf{u}_h$ in Eq. 31 and treating the right-hand side using Eqs. 85–87, and 90 of Lemma 3, we get:

$$\sum_{E\in\tau_h}(1-\epsilon_1-\frac{\kappa_E}{\epsilon_2}-\frac{\kappa_E}{\alpha\epsilon_4})\int_E K^{-1}\mathbf{u}_h\cdot\mathbf{u}_h\,\mathrm{d}x$$
$$+\sum_{e\in\xi_h^{\mathrm{N}}}\frac{1-\epsilon_3}{\alpha}\int_e(\mathbf{u}_h\cdot\mathbf{n}_e)^2\,\mathrm{d}\gamma$$
$$\leq\sum_{E\in\tau_h}\frac{1}{4\epsilon_1}\int_E K\nabla p_h\cdot\nabla p_h\,\mathrm{d}x+\sum_{e\in\xi_h'}\epsilon_2\int_e[\![p_h]\!]^2\,\mathrm{d}\gamma$$
$$+\sum_{e\in\xi_h^{\mathrm{D}}}\epsilon_2\int_e(p_h-p_{\mathrm{D}})^2\,\mathrm{d}\gamma+\sum_{e\in\xi_h'}\int_e\frac{\epsilon_4}{2\alpha}\,\mathrm{d}\gamma[\![K\nabla p_h\cdot\mathbf{n}_e]\!]^2$$
$$+\sum_{e\in\xi_h^{\mathrm{N}}}\frac{1}{4\epsilon_3\alpha}\int_e(g_{\mathrm{N}})^2\,\mathrm{d}\gamma\tag{92}$$

Hence the required stability holds provided there exist two constants c_1 and c_2 such that

$$\begin{cases}1-\epsilon_1-\dfrac{\kappa_E}{\epsilon_2}-\dfrac{\kappa_E}{\alpha\epsilon_4}>0,\\ 1-\epsilon_3>0,\\ \dfrac{1}{4\epsilon_1}\leq 1,\\ 2\epsilon_2=c_1\times\beta,\\ \epsilon_4\beta=c_2\times\alpha,\end{cases}$$

where β is the one used when solving pressure equation. Treating all these constraints shows that α should depend on β. More precisely, take $c_2=1$ and rename $c_1=a$, we get $\epsilon_2=a\beta$, and $\alpha=\epsilon_4\beta$. We need then to select $\epsilon_1, a, \epsilon_4$, such that

$$\frac{1}{4}\leq\epsilon_1<1-\kappa_E\left(\frac{1}{\epsilon_2}+\frac{1}{\alpha\epsilon_4}\right).$$

This will be the case if we can find them such that

$$\frac{\kappa_E}{\beta}\left(\frac{1}{a}+\frac{1}{\epsilon_4^2}\right)<\frac{3}{4}.$$

Since $\frac{3\beta}{4\kappa_E}$ is constant, we can always find $a>0$ such that $\frac{3\beta}{4\kappa_E}-\frac{1}{a}>0$ and consequently determine ϵ_4 by

$$\epsilon_4 \geq \frac{1}{\sqrt{\frac{3\beta}{4\kappa_E}-\frac{1}{a}}}$$

and the result holds. □

This proof shows that when we have determined $a>0$ such that $\frac{3\beta}{4\kappa_E}-\frac{1}{a}>0$, then we can define α in problem (31) by

$$\alpha \geq \frac{\beta}{\sqrt{\frac{3\beta}{4\kappa_E}-\frac{1}{a}}}.$$

Appendix 7: Proof of Proposition 6

Proof Taking $\mathbf{v}_h=\mathbf{u}_h$ in Eq. 37 and treating the right-hand side using Eqs. 85–90 of Lemma 3, we get:

$$\begin{aligned}
&\sum_{E\in\tau_h}\left(1-\epsilon_1-\frac{\kappa_E}{\epsilon_2}\right)\int_E K^{-1}\mathbf{u}_h\cdot\mathbf{u}_h\,\mathrm{d}x\\
&+\sum_{e\in\xi_h'}\frac{1}{4\alpha}\left(1-\frac{1}{4\epsilon_4}\right)\int_e[\![\mathbf{u}_h\cdot\mathbf{n}_e]\!]^2\,\mathrm{d}\gamma\\
&+\sum_{e\in\xi_h'}\frac{1}{\alpha}\left(1-\frac{1}{4\epsilon_5}\right)\int_e\{\mathbf{u}_h\cdot\mathbf{n}_e\}^2\,\mathrm{d}\gamma\\
&+\sum_{e\in\xi_h^{\mathrm{N}}}\frac{1-\epsilon_3}{\alpha}\int_e(\mathbf{u}_h\cdot\mathbf{n}_e)^2\,\mathrm{d}\gamma\\
&\leq\sum_{E\in\tau_h}\frac{1}{4\epsilon_1}\int_E K\nabla p_h\cdot\nabla p_h\,\mathrm{d}x+\sum_{e\in\xi_h'}\epsilon_2\int_e[\![p_h]\!]^2\,\mathrm{d}\gamma\\
&\quad+\sum_{e\in\xi_h^{\mathrm{D}}}\epsilon_2\int_e(p_h-p_{\mathrm{D}})^2\,\mathrm{d}\gamma\\
&\quad+\sum_{e\in\xi_h'}\frac{\epsilon_4}{4\alpha}\int_e[\![K\nabla p_h\cdot\mathbf{n}_e]\!]^2\,\mathrm{d}\gamma\\
&\quad+\sum_{e\in\xi_h'}\frac{\epsilon_5}{\alpha}\int_e\{K\nabla p_h\cdot\mathbf{n}_e\}^2\,\mathrm{d}\gamma\\
&\quad+\sum_{e\in\xi_h^{\mathrm{N}}}\frac{1}{4\epsilon_3\alpha}\int_e(g_{\mathrm{N}})^2\,\mathrm{d}\gamma. \qquad (93)
\end{aligned}$$

Hence, the required stability holds provided there exist two constants c_1, c_2, and c_3 such that

$$\begin{cases}
1-\epsilon_1-\dfrac{\kappa_E}{\epsilon_2}>0, & 1-\dfrac{1}{4\epsilon_4}>0,\\
1-\dfrac{1}{4\epsilon_5}>0, & 1-\epsilon_3>0,\\
\dfrac{1}{4\epsilon_1}\leq 1, & 2\epsilon_2=c_1\times\beta,\\
\epsilon_4\beta=c_2\times\alpha, & \epsilon_5\beta=c_3\times\alpha.
\end{cases}$$

Treating this as above shows that α is independent of β. More precisely, since $\frac{\kappa_E}{\beta}$ and $\frac{\beta}{\alpha}$ are constants, by taking $c_1>\frac{8\kappa_E}{3\beta}$, $c_2>\frac{\beta}{\alpha}$ and $c_3>\frac{\beta}{\alpha}$, it is possible to determine ϵ_i, $i=1,2,3,4,5$ such that the above constraints are satisfied. Consequently, α in problem (37) is independent of β. □

References

1. Adams, R.A., Fournier, J.J.F.: Sobolev spaces. In: Pure Appl. Math (Amsterdam), vol. 140, 2nd edn. Elsevier/Academic, Amsterdam (2003)
2. Arnold, D.N., Brezzi, F., Cockburn, B., Marini, D.: Discontinuous Galerkin methods for elliptic problems. In: Cockburn, B., Karniadakis, G.E., Shu, C.W. (eds.) Discontinuous Galerkin Methods. LNCSE, vol. 11, pp. 89–101, Springer, New York (2000)
3. Arnold, D.N., Brezzi, F., Cockburn, B., Marini, D.: Unified analysis of discontinuous Galerkin methods for elliptic problems. SIAM J. Numer. Anal. **39**(5), 1749–1779 (2001)
4. Arnold, D.N., Brezzi, F., Cockburn, B., Marini, L.: Unified analysis of discontinuous Galerkin methods for elliptic problems. SIAM J. Numer. Anal. **39**(5), 1749–1779 (2002)
5. Babuška, I., Baumann, C.E., Oden, J.T.: A discontinuous *hp* finite element method for diffusion problems: 1-D analysis. Comput. Math. Appl. **37**, 103–122 (1999)
6. Bastian, P., Lang, S.: Couplex benchmark computations with UG. Comput. Geosci. **8**(2), 125–147 (2004)
7. Bastian, P., Rivière, B.: Superconvergence and $H(\mathrm{div})$ projection for discontinuous Galerkin methods. Int. J. Numer. Methods Fluids **42**(10), 1043–1057 (2003)
8. Bourgeat, A., Kern, M., Schumacher, S., Talandier, J.: The Couplex test cases: nuclear waste disposal simulation (2002). http://www.gdrmomas.org/Ex_qualif/Couplex/Documents/couplexall.pdf. Unpublished
9. Brezis, H.: Analyse fonctionnelle. Collection Mathématiques Appliquées pour la Maîtrise. [Collection of Applied Mathematics for the Master's Degree]. Masson, Paris (1983). Théorie et applications. [Theory and applications]
10. Brezzi, F., Cockburn, B., Marini, L.D., Süli, E.: Stabilization mechanisms in discontinuous Galerkin finite element methods. Comput. Methods Appl. Mech. Eng. **195**(25–28), 3293–3310 (2006)
11. Brezzi, F., Douglas, J.J., Marini, L.D.: Recent results on mixed finite element methods for second order elliptic problems. Istituto di Analisi Numerica del Consiglio Nazionale delle Ricerche [Institute of Numerical Analysis of the National Research Council], vol. 431. Istituto di

Analisi Numerica del Consiglio Nazionale delle Ricerche, Pavia (1984)
12. Brezzi, F., Hughes, T.J.R., Marini, L.D., Masud, A.: Mixed discontinuous Galerkin methods for Darcy flow. J. Sci. Comput. **22/23**, 119–145 (2005)
13. Castillo, P.: An optimal error estimate for the local discontinuous Galerkin method. In: Cockburn, B., Karniadakis, G.E., Shu, C.W. (eds.) Discontinuous Galerkin Methods, pp. 285–290. Springer, New York (2000)
14. Castillo, P.: Local discontinuous Galerkin methods for convection–diffusion and elliptic problems. Ph.D. thesis, University of Minnesota, Minneapolis (2001)
15. Castillo, P., Cockburn, B., Perugia, I., Schötzau, D.: An a priori error estimate of the local discontinuous Galerkin method for elliptic problems. SIAM J. Numer. Anal. **38**(5), 1676–1706 (2000)
16. Cockburn, B., Kanschat, G., Perugia, I., Schötzau, D.: Superconvergence of the local discontinuous Galerkin method for elliptic problems on Cartesian grids. SIAM J. Numer. Anal. **39**(1), 264–285 (2001)
17. Cockburn, B., Karniadakis, G.E., Shu, C.W. (eds.): Discontinuous Galerkin methods. In: Lecture Notes in Computational Science and Engineering, vol. 11. Theory, Computation and Applications, Papers from the 1st International Symposium held in Newport, RI, 24–26 May 1999. Springer, Berlin (2000)
18. Cockburn, B., Shu, C.W.: The local discontinuous Galerkin method for time-dependent convection–diffusion systems. SIAM J. Numer. Anal. **35**, 2440–2463 (1998)
19. Ern, A., Nicaise, S., Vohralík, M.: An accurate **H**(div) flux reconstruction for discontinuous Galerkin approximations of elliptic problems. C. R. Math. Acad. Sci. Paris **345**(12), 709–712 (2007)
20. Gilbarg, D., Trudinger, N.S.: Elliptic Partial Differential Equations of Second Order. Classics in Mathematics. Springer, Berlin (2001). Reprint of the 1998 edition
21. Hughes, T.J.R., Masud, A., Wan, J.: A stabilized mixed discontinuous Galerkin method for Darcy flow. Comput. Methods Appl. Mech. Eng. **195**(25–28), 3347–3381 (2006)
22. Kanschat, G.: Preconditioning methods for local discontinuous Galerkin discretizations. SIAM J. Sci. Comput. **25**(3), 815–831 (2003)
23. Marini, D.: A survey of DG methods for elliptic problems. In: Brezzi, F., Buffa, A., Corsaro, S., Murli, A.(eds.) Numerical Mathematics and Advanced Applications: ENUMATH 2001, pp. 805–814. Springer Italia, Milan (2003)
24. Naff, R.L., Russell, T.F., Wilson, J.D.: Shape functions for velocity interpolation in general hexahedral cells. Comput. Geosci. **6**(3–4), 285–314 (2002); Locally conservative numerical methods for flow in porous media
25. Raviart, P.A., Thomas, J.M.: A mixed method for second order elliptic problems. In: Galligani, I., Magenes, E. (eds.) Mathematical Aspects of the Finite Element Method. Springer, New York (1977)
26. Rivière, B.: Discontinuous Galerkin methods for solving the miscible displacement problem in porous media. Ph.D. thesis, University of Texas at Austin (2000)
27. Rivière, B., Wheeler, M.F., Girault, V.: Improved energy estimates for interior penalty, constrained and discontinuous Galerkin methods for elliptic problems. I. Comput. Geosci. **3**(3–4), 337–360 (2000) (1999)
28. Sun, S.: Discontinuous Galerkin methods for reactive transport in porous media. Ph.D. thesis, University of Texas at Austin (2003)
29. Sun, S., Wheeler, M.F.: Discontinuous Galerkin methods for coupled flow and reactive transport problems. Appl. Numer. Math. **52**(2–3), 273–298 (2005)
30. Sun, S., Wheeler, M.F.: Symmetric and nonsymmetric discontinuous Galerkin methods for reactive transport in porous media. SIAM J. Numer. Anal. **43**(1), 195–219 (2005)
31. Warburton, T., Hesthaven, J.S.: On the constants in *hp*-finite element trace inverse inequalities. Comput. Methods Appl. Mech. Eng. **192**(25), 2765–2773 (2003)
32. Zienkiewicz, O.C., Zhu, J.Z.: The superconvergent patch recovery and a posteriori error estimates. I. The recovery technique. Int. J. Numer. Methods Eng. **33**(7), 1331–1364 (1992). doi:10.1002/nme.1620330702